PROCESSES CONTROLLING THERMOKARST LAKE EXPANSION RATES ON THE ARCTIC COASTAL PLAIN OF NORTHERN ALASKA

By

Allen C. Bondurant, B.S.

A Thesis Submitted in Partial Fulfillment of the Requirements for the Degree of

MASTER OF SCIENCE

In

Geoscience: Interdisciplinary Program

University of Alaska Fairbanks

August 2017

APPROVED:

Christopher D. Arp, Committee Chair

Benjamin M. Jones, Committee Member

Ronald P. Daanen, Committee Member

Yuri L. Shur, Committee Member

J. Leroy Hulsey, Chair

Department of Civil & Environmental Engineering

Douglas J. Goering, Dean

College of Engineering and Mines

Michael A. Castellini, *Dean of the Graduate School*

Abstract:

Thermokarst lakes are a dominant factor of landscape scale processes and permafrost dynamics in the otherwise continuous permafrost region of the Arctic Coastal Plain (ACP) of northern Alaska. Lakes cover greater than 20% of the landscape on the ACP and drained lake basins cover an additional 50 to 60% of the landscape. The formation, expansion, drainage, and reformation of thermokarst lakes has been described by some researchers as part of a natural cycle, the thaw lake cycle, that has reworked the ACP landscape during the course of the Holocene. Yet the factors and processes controlling contemporary thermokarst lake expansion remain poorly described. This thesis focuses on the factors controlling variation in extant thermokarst lake expansion rates in three ACP regions that vary with respect to landscape history, ground-ice content, and lake characteristics (i.e. size and depth). Through the use of historical aerial imagery, satellite imagery, and field-based data collection, this study identifies the controlling factors at multiple spatial and temporal scales to better understand the processes relating to thermokarst lake expansion. Comparison of 35 lakes across the ACP shows regional differences in expansion rate related to permafrost ice content ranging from an average expansion rate of 0.62 m/yr on the Younger Outer Coastal Plain where ice content is highest to 0.16 m/yr on the Inner Coastal Plain where ice content is lowest. Within each region, lakes vary in their expansion rates due to factors such as lake size, lake depth, and winter ice regime. On an individual level, lakes vary due to shoreline characteristics such as local bathymetry and bluff height. Predicting how thermokarst lakes will behave locally and on a landscape scale is increasingly important for managing habitat and water resources and informing models of land-climate interactions in the Arctic.

Table of Contents

List of Figures

Page

List of Tables

Page

Preface

This thesis consists of a single chapter aimed to further study the dynamics of thermokarst lakes on the Arctic Coastal Plain of Alaska, written to fulfill the graduation requirements for an interdisciplinary Master of Science, concentrating in Geoscience, from the University of Alaska Fairbanks College of Engineering and Mines, Civil & Environmental Engineering Department. I began this work in January of 2015, developing a study design and beginning analysis with the input of Christopher Arp and Benjamin Jones. I was the lead for conducting field work, remote sensing analysis, and writing of the manuscript.

Funding for this study was provided by NSF Grant ARC-1417300. This work benefitted from the U.S. Geological Survey and Woods Hole Coastal Marine Science Center and their Digital Shoreline Analysis System tool, as well as the U.S. Geological Survey Earth Resources Observation and Science Center for their imagery archive. European Space Agency Copernicus Sentinel Data 2016 was retrieved from the Alaska Satellite Facility DAAC.

I would like to thank my graduate advisor Dr. Christopher Arp for providing me with the opportunity to study these arctic lakes as a Masters student, and to travel and work in such amazing country. In addition, I would also like to thank my other committee members Drs. Benjamin Jones, Yuri Shur, and Ronald Daanen. Their guidance proved invaluable to me during my project. I also thank Mikhail Kanevskiy, Carson Baughman, and Melanie Engram for their expertise and assistance. I must finally thank my family for always supporting my academic career, particularly over these past two years.

1. Introduction

Thermokarst lakes are abundant landforms of permafrost regions, particularly in lowland areas with high ground ice content. Initiating as depressions by some surface disturbance formed by thawing of ice rich permafrost (van Everdingen, 1998), thermokarst depressions fill with water causing ponds to gradually expand and coalesce to often form large lakes. The abundance and dynamic nature of thermokarst lakes makes these landforms play a dominant role in landscape processes, such as surface energy balance, permafrost dynamics, hydrologic storage and export, carbon cycling, and provision of habitat for fish and water birds. Perhaps foremost, lakes set in permafrost create as a major thermal departure in the ground thermal regime (Brewer, 1958; Lachenbruch et al., 1962; Ling and Zhang, 2003). The warm mean annual temperature of the lakes compared to their surroundings contributes to permafrost thaw, which though localized to the lake, becomes regionally important with the cumulative density of lakes (Grosse et al., 2013). This thaw also contributes to the release of stored permafrost carbon in the form of carbon dioxide and methane (Zimov et al., 1997), contributing a source of atmospheric carbon to the global carbon budget (Walter et al., 2006). As the dominant landscape feature in arctic lowlands, they also play a controlling role in regional hydrology. In this low gradient landscape, lakes act as the primary form of surface storage, where summer evapotranspiration (ET) exceeds summer precipitation. They act in routing and intercepting spring snowmelt runoff, maintaining the water balance lost to ET the prior summer (Rovansek, 1996; Bowling et al., 2003) and relating to snowmelt and baseflow recession hydrologic regimes (Arp et al., 2012b). Their role in hydrologic storage also serves as a residential water source for many communities across northern Alaska, Canada, and Russia (Boyd, 1959; Dmitriev and Tolstikhin, 1971; Heinke and Deans, 1973; Martin et al., 2007; Alessa et al., 2008), as well as a water source for infrastructure tied to resource development, including ice roads (Sibley et al., 2008; Jones et al., 2009). Thermokarst lakes provide important

habitat for fish and migratory birds making lake-rich regions of Arctic lowlands highly productive landscapes (Alerstam et al., 2001), which in turn support local fisheries and subsistence hunting and migratory waterbird harvest throughout the lower latitudes (Vincent and Hobbie, 2000; Berkes and Jolly, 2001).

Lakes are spatially distributed across much of the northern high latitudes, with the highest concentration of lakes on Earth occurring between 50° - 70° N (Lehner and Döll, 2004), largely due to the presence of permafrost or to a history of glaciation. Thermokarst lakes, specifically, then are found in any lowland permafrost region with high ground ice content and a thick sediment package, a terrain susceptible to their formation. This includes broad swaths of land across Siberian Russia, Northwest Canada, and Interior and Northern Alaska (Grosse et al., 2013). As a region with high ground ice contents that was not glaciated during the last glacial maximum, thermokarst lakes dominate the Arctic Coastal Plain of Alaska, covering greater than 20% of land area (Sellmann et al., 1975; Hinkel et al., 2005, Arp & Jones, 2009).

Thermokarst lakes are highly dynamic landscape features, continuously evolving and interacting with the surrounding landscape. The classic thermokarst or "thaw" lake cycle begins with a surface disturbance initiating permafrost degradation and thaw subsidence which initiates a water-filled depression (Cabot, 1947; Britton, 1957; Carson, 1968; Everett, 1980;). Small ponds that form through this process continue to expand and coalesce, eventually forming larger lakes with progressively deepening basins (Britton, 1957; Carson, 1968) and thawed sub-lake permafrost or a talik if/when the mean annual lake bottom temperature exceeds 0°C (Brewer, 1958; Lachenbruch, 1962; West and Plug, 2008; Arp et al., 2016). Eventually thermokarst lakes can drain catastrophically through a variety of internal (e.g., lake expansion across lower margins or overtopping and downcutting through ice wedge networks) and external (e.g., erosional capture

by a lower elevation stream, lake, or coastline) mechanisms, leaving a partly or completely drained thermokarst lake basin (DTLB) (Hopkins, 1949; Carson & Hussey, 1962; Mackay, 1988; Brewer et al., 1993; Hinkel et al., 2007; Marsh et al., 2009; Jones and Arp, 2015). Newly formed DTLBs are then susceptible to permafrost aggradation and ice-wedge formation, at which point the cycle may start again if ice-rich permafrost degrades and small ponds develop that coalesce and expand over time (Carson, 1968; Everett, 1980; Billing and Peterson, 1980). Jorgenson and Shur (2007) expand on this model to include an alternative lake evolution trajectory on the ACP because of the short timelines implied by prior literature and the lack of sufficient ground ice to allow thaw lake redevelopment. In all concepts of thermokarst lake evolution, shoreline erosion and lateral expansion are seen as key processes determining local and regional variation in the thaw lake cycle and how thermokarst lakes will respond to changes in climate.

The processes by which thermokarst lakes expand, vary depending upon the dominant climate driven forces and environmental controls at play. These forces express themselves across various spatial and temporal scales, and it is this network of interactions that contribute to the heterogeneity of shoreline expansion in thermokarst lakes. At the regional scale, the local geology and climate conditions likely serve as the strongest controls on shoreline expansion rates. Warm ground temperatures or high ice contents would be considered driving forces behind thermokarst lake expansion at the landscape scale. For a particular lake, the lake size, lake depth, wave energy, bluff height, lake-marginal permafrost temperature, and terrain units are likely factors that control lake expansion. Additional factors that likely promote erosional susceptibility include ice content, organic matter content and soil cohesion, and soil temperatures. Factors that limit erosional

susceptibility would include basin morphologies that limit wind and wave fetch, length of open water season, and location on the lake respective to prevailing wind direction.

Several key processes likely dictate variability in thermokarst lake expansion rates at local and regional scales. In areas with steep banks and high massive ice content, this can include the formation of thermo-erosional niches and subsequent block collapse (Fig. 1a). Areas with gentler slopes but high ice contents are susceptible to thaw slumping and other thermally associated mass wasting action including thermal denudation (Fig. 1b) and active layer detachments. Low lying bluffs can be subject to mechanical erosion by wave action, ice wedge degradation along polygon troughs (Fig. 1d), and ice shove processes during spring break up (Fig. 1c) (Mackay, 1970; Kobayashi, 1985; Kokelj, 2009; Kovacs, 1983). Lake characteristics can vary at different points along their perimeter due to differential lake bathymetry, different local terrain units, and different bluff heights, therefore all of these processes can potentially occur on the same lake, at the same time, depending on conditions like wind direction, water and permafrost temperature, and variations within bluff morphology and content. This variation in conditions and erosional process likely leads to varying expansion rates in thermokarst lakes.

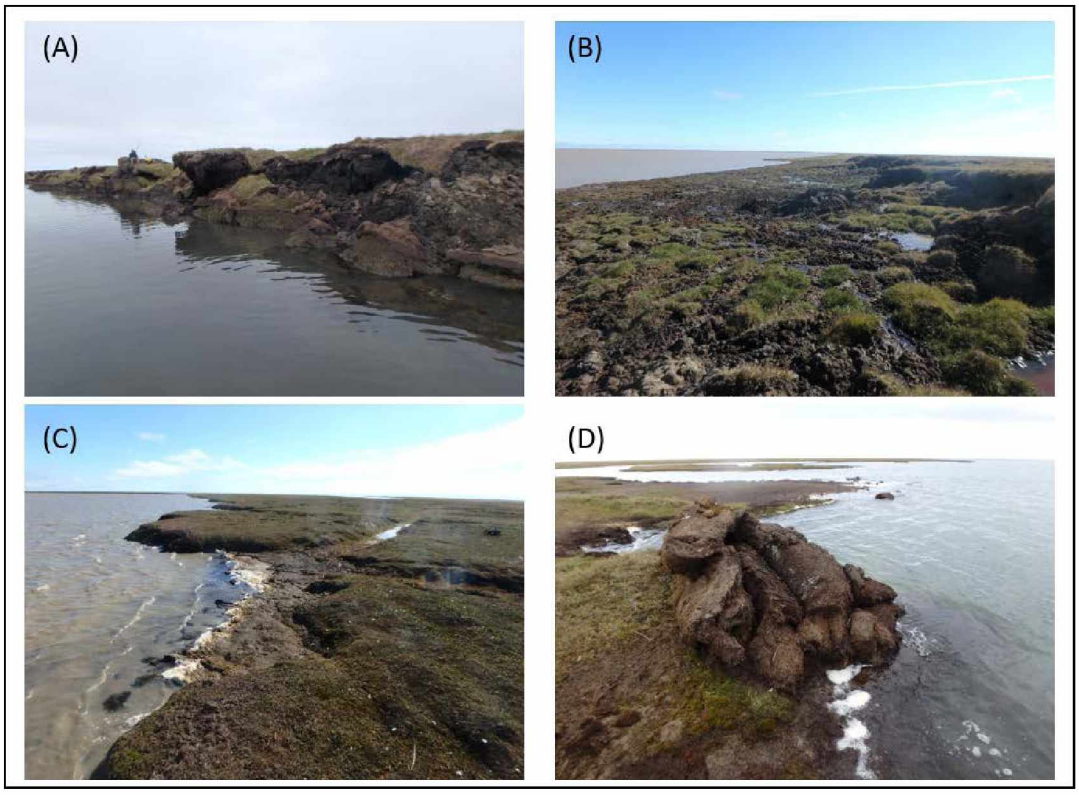

Figure 1: Examples of shoreline erosional features: (a) thermo-erosional niche formation and block collapse (b) thermal demudation (c) ice wedge degradation (d) ice shove

Models of shoreline expansion on the ACP have previously focused on the salient orientation of lakes aligned 10° - 15° west of true north. The currently accepted hypothesis behind this orientation, after having gone through several iterations, is that prevailing winds cause circulation patterns within the lake, influencing wave action nearly normal to the axis of orientation, accumulate insulating sublittoral shelves on the east and west shores while preferentially eroding the more exposed north and south shores (Black and Barksdale, 1949; Livingstone, 1954; Carson and Hussey, 1962). The aggraded sand and organic material of these sublittoral shelves serves to both insulate the underlying permafrost and to physically armor it against wave erosion. In this way they serve as a strong resisting force to lakeshore expansion. The circulation patterns that cause this deposition, direct wave energy towards the northern and

southern ends of the lake and act as a driving force for this same expansion, without the benefit of the more resistive shores with peat deposits.

This wind-driven lake orientation hypothesis largely neglects wintertime processes, however, and the effect they may have on lake shore expansion. Sturm and Liston (2003) hypothesize that these winds also play a role in these wintertime processes. By scouring snow on the eastern shores of these lakes, the prevailing winter winds serve to armor the shorelines by more solidly freezing the banks and bed in these locations, resisting thermal and mechanical erosion later into the summer. If the Arctic experiences potentially snowier conditions in the future (Serreze et al., 2000; Wendler et al., 2014), this effect could become more pronounced in a changing climate. Wintertime processes extend beyond snow distribution, however. The depth of a lake, whether it freezes to the bottom or not, and its mean annual bed temperature are important aspects to consider. On the ACP where lakes are experiencing thinner ice growth and lakes transition from bedfast to floating ice regimes (Arp et al., 2012a; Surdu et al., 2014; Alexeev et al. 2016), the role of wintertime processes thus may become increasingly important for understanding lake change processes and how some ACP thermokarst lakes become reshaped over time.

Most thermokarst lakes on the ACP are shallow due to their formation in permafrost with high ice content only near the surface, particularly on the outer coastal plain (Jorgenson and Shur, 2007). Because lake depths are often close to the maximum thickness of seasonal ice, many freeze solid with bedfast ice and other slightly deeper lakes retain liquid water below floating ice (Brewer, 1958; Lachenbruch et al., 1962, Mackay, 1992; West and Plug, 2008, Arp et al., 2011). The lake depth separating these ice regimes generally exists somewhere between 1.5 m and 2 m, where maximum winter ice growth is reached by the end of winter (Brewer, 1958; Sellmann et. al. 1975), though evidence suggest a trend toward thinner maximum ice thickness and a shift toward more

floating ice conditions (Arp et al. 2012a; Surdu et al. 2014).. The most critical effect created by floating ice conditions is the distinctly warmer thermal regime of a lake bed that leads to development of a thaw-bulb (talik) (Lachenbruch, 1962; West & Plug, 2008). The thermal impact generated by floating ice conditions may also occur laterally into surrounding lake shorelines and bluffs (Arp et al. 2011; Langer et al. 2016). In lakes with bedfast ice regimes, warming of the permafrost can still occur and may be becoming more rapid as trends in thinning lake ice increases floating lake ice conditions (Arp et al. 2016). The extent to which warmer sublake permafrost is also apparent along shorelines is uncertain, but evidence from other continuous permafrost regions suggest a similar response (Roy-Léveillée and Burn, 2017) to lake centers, where perennially thawed ground will not exist due to the presence of liquid water year round and mean annual temperatures greater than 0°C (Brewer, 1958; Lachenbruch, 1962; West & Plug, 2008). Since permafrost temperatures are colder beneath and adjacent to bedfast ice lakes relative to floating ice lakes, they may be less susceptible to thermal erosion, which would be manifest in lower overall thermokarst lake expansion rates. This pattern was observed by Arp et al. (2011), with bedfast ice lakes within the YOCP showing lower expansion rates than floating ice lakes over the time period 1979-2002. Another difference between bedfast and floating ice regimes was noted in Arp et al. (2011) that showed that bedfast ice lakes are preferentially eroding at their northern and southern ends compared to floating ice lakes, which had more even patterns of erosion in all directions. This observed oriented expansion in bedfast lakes likely contributes to the orientation of lakes on the outer ACP.

The lack of consensus over lakeshore expansion processes, controls, and decadal-scale rates underscores the need to further understand the forces controlling where, when, and to what extent thermokarst lake expansion occurs. This thesis addresses the potential impact of regional

geology, including ground ice content and soil characteristics, through the analysis of 35 lakes in three distinct regions on the ACP. The impacts of localized factors, including lake ice regime, snow accumulation, and bluff height and slope on the processes that contribute to thermokarst lake expansion rates are addressed through comparisons within an individual region and within an individual lake. I hypothesize that lakes will predominantly be controlled by their regional setting and ice conditions, with wintertime processes playing a larger role than previously considered. Through a multi-scale approach using remote sensing techniques in addition to field based data collection, this analysis aims to better inform those involved in land and water resource management on the ACP as to the dynamics of lake expansion processes.

2. Study Area and Design

The main study area for this research (Figure 2) is the Arctic Coastal Plain of northern Alaska. This region of Alaska includes numerous lakes in various stages of development, from small thaw ponds initiated in drained thermokarst lake basins (DTLB) to large, mature lakes expanding into their surroundings through shoreline erosion. These lakes cover >20% of the land area on the outer ACP. Those areas which are not present day lakes often show characteristics and morphology of drained thermokarst lake basins or remnant uplands (Jorgenson and Brown, 2005; Jones and Arp, 2015), providing evidence that lake shoreline expansion processes have been occurring for long periods of time (Hinkel et al., 2003). The tundra (DTLBs and remnant uplands) is characterized by the presence of high and low centered ice wedge polygons. The surficial geology consists of continuous permafrost composed of glacio-marine sandy/silty sediments with high ice contents ranging from 70% to 86% in the upper 1-2 m and 20% in the upper 20m (Brown, 1968; Sellmann et al 1975, Kanevskiy et al., 2013). Permafrost temperatures in this area are

approximately -7 °C (Urban & Clow, 2015). Elevations range from sea level to 13 m asl, with little topography except lake bluffs. Prevailing winds are from the ENE. The region has an Arctic climate with mean annual air temperatures around -10 °C. The region typically experiences 15-20 cm centimeters of precipitation per year (Shulski and Wendler, 2007). Landscape drainage networks are complex due to the low relief, high lake cover, and impermeability of permafrost soils (Roulet and Woo, 1988; Bowling et al., 2003; Arp et al., 2012b). Most lakes are connected to this network and act in routing snowmelt and rainfall. Ice cover persists on lakes from September to July (Arp et al., 2011) and historically experience maximum ice thicknesses of about 2 m. This creates a functional difference between lakes that experience bedfast ice conditions and floating ice conditions. This difference represents a first order control on the thermal state of the permafrost beneath lakes (Brewer, 1958; Lachenbruch, 1962; Sellmann et al., 1975; Ling and Zhang, 2003; Arp et al., 2011; Arp et al., 2012a).

Three study areas were chosen according to the differences in surficial geology and lake characteristics on the ACP (Table 1). The OCP study area located on the Barrow Peninsula (Figure 2) is among the most well studied in the Alaskan Arctic, and consists of a surficial package referred to as the Outer Coastal Plain (OCP) deposit (Williams et al., 1978; Hinkel et al., 2005). The OCP terrain is a marine sand deposited in multiple Pleistocene and Pliocene marine transgressions (Dinter et al., 1990) with surfaces 7-23 m asl. Volumetric ice contents (VIC) for this deposit averages 80% (Kanevskiy et al., 2013) and mean annual soil temperature (MAST) at 1.2 m depth was -7.3 °C over the period of 1999-2010 (Urban & Clow, 2015; Farquharson et al. 2016). Vegetation consists of mixed sedges and mosses typical of moist acidic tussock tundra, with some dwarf shrubs (Raynolds et al., 2006). Lakes on the Barrow Peninsula have a strong and

predominant orientation 7° NNW and have an average size of 45 ha, with length to width ratios greater than 2 (Hinkel et al. 2005).

The YOCP study area (Figure 2) is located in the northern portion of the Teshekpuk Lake Special Area (TLSA) and the northeastern portion of the Barrow Peninsula and consists of a younger deposit referred to as the Younger Outer Coastal Plain (YOCP) which was left behind by the Simpsonian transgression approximately 78-58 kya with surfaces 0-7 m asl (Carter et al. 1988, Dinter et al. 1990). Glacio-marine silty sediments susceptible to the aggradation of high volumes of ground ice were deposited here. Thus, ice contents of the upper three meters of permafrost here are higher than the OCP region and average 86% VIC (Kanevskiy et al., 2013; Farquharson et al. 2016). Vegetation is similar to the OCP, but with the absence of dwarf shrubs (Raynolds et al. 2006). At the Drew Point climate station within the YOCP, permafrost temperatures here are slightly colder than the OCP, with a MAST at 1.2 m depth of -8.0 °C between 1999 and 2010 (Urban & Clow, 2015; Farquarson et al. 2016). Mean lake size within this deposit is 143 ha, and lakes cover 18% of the land surface, if Teshekpuk Lake itself is excluded. Lakes here also show strong orientation of their long axis at 9° NNW, and have a strongly elliptical fit, though slightly less so than the OCP Region (Hinkel et al. 2005).

The ICP study area (Figure 2) is located in the lower Fish Creek Watershed (FCW) and differs from the other two study regions in that it is underlain predominantly by a marine sand deposit to the east of the study area and by an aeolian sand deposit to the west, collectively referred to as the Inner Coastal Plain (ICP) unit (O'Sullivan, 1961; Williams et al., 1978; Carter, 1981; Williams, 1983). These coarser grained materials do not allow for the same aggradation of ground ice, and VIC ground ice contents range between 45% to 71% for this region (Jorgenson and Shur, 2007; Kanevskiy et al., 2013; Farquharson et al. 2016). Lakes cover 18% of land surface area for

this unit with a mean size of 40 ha. Though these lakes do show orientation of their long axis in the same directions as the other two units, at approximately 10° NNW, they are not as strongly elliptical as those lakes within each of the other units (Hinkel et al. 2005).

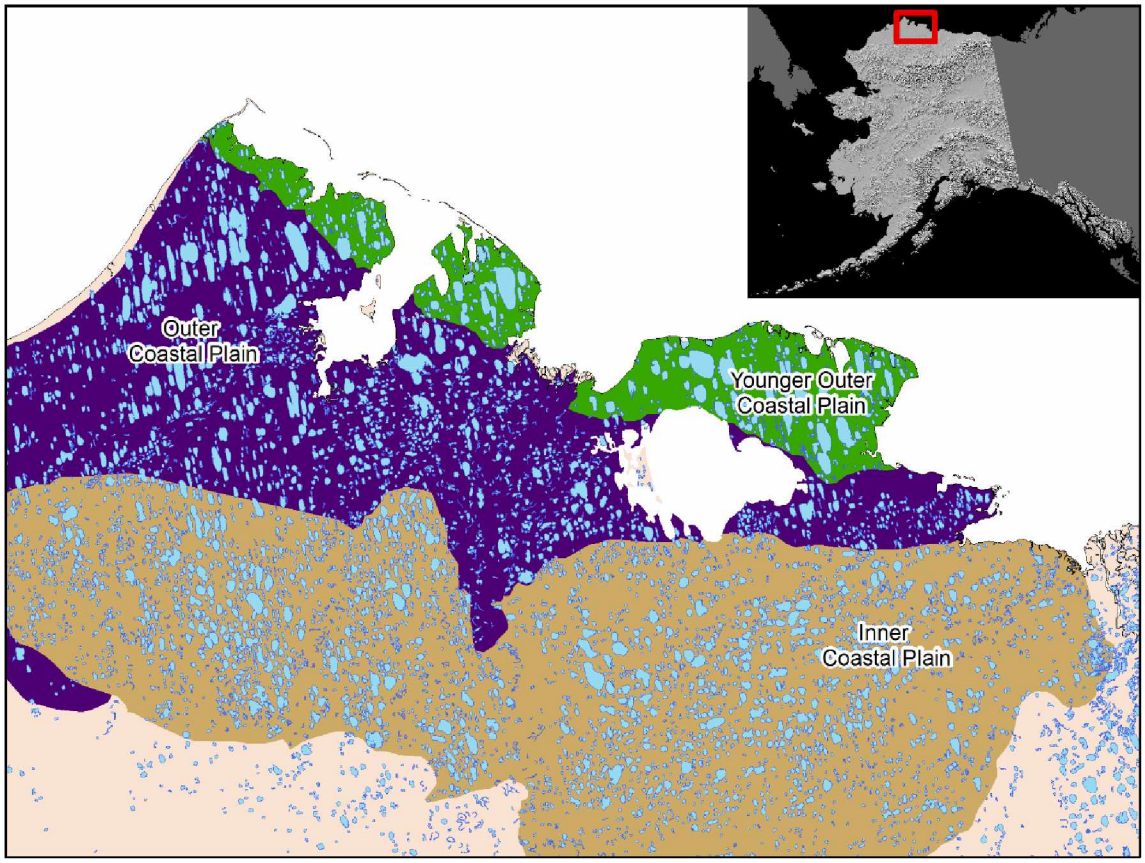

Figure 2: This map shows the different regions in this study, split by quaternary geology. To the north is the Younger Outer Coastal Plain (YOCP) Unit, in the center] is the Outer Coastal Plain (YOCP) Unit, and to the south is the Inner Coastal Plain (ICP) Unit. The inset shows the location of the study area in the state of Alaska.

Table 1: Summary of characteristics for each study region within the broader Arctic Coastal Plain.

Region	YOCP	OCP	ICP
Elevation (m asl)	0-5	1-9	4-25
Dominant Surface Geology [Hinkel et al., 2005]	Glacio-Marine Silt	Glacio-Marine Sand/Silt	Marine Sand and Silt
Ground Ice Content (Volumetric) [Kanevskiy, 2013]	86%	80%	71%
Lake Area % [Hinkel et al., 2005]	22.6	18.0	17.8
Dominant Lake Orientation (°NNW) [Hinkel et al., 2005]	11°	7°	10°
MAGT at 1.2 m depth (°C) [Urban & Clow, 2015]	-8	-7.3	-6.9

These regions were also chosen in part because of the length of the scientific record in each area. These areas have a history of scientific research beginning in 1948 with the establishment of the Naval Arctic Research Laboratory (NARL) in Barrow, AK with the task of conducting research throughout what was then known as the Naval Petroleum Reserve No. 4, now known as the National Petroleum Reserve-Alaska (NPR-A) (Shelesnyak, 1948). NARL laid the foundation for research on the ACP, studying the lakes and permafrost across many miles of remote tundra, but was also key in establishing logistical bases of operation that are crucial to this day, in the form of research laboratories in Barrow and the remote research cabin situated within the TLSA. Aerial photography exists from the efforts of NARL and the USGS from the 1940s and 1950s along the ACP, allowing for examination of erosion rates over a several decade time period when compared to more recent image acquisitions. The climate data record is also strong for each of these

locations. Barrow's climate record extends uninterrupted to 1921 and is the longest continuous temperature record in the Alaskan Arctic (Hamilton, 1965). Weather stations have been continuously monitoring conditions both in the TLSA and FCW since 1998, giving additional spatial distribution of climate conditions with a solid record (Urban & Clow, 2015). Finally, lakes in each of these areas have been the objects of intensive monitoring for the past four years or more as parts of various long term observation studies including the Circum-Arctic Lake Observation Network (CALON), providing information on lake morphology, ice thickness records, water levels, and lake bed temperature (Hinkel et al. 2012; Arp et al. 2015). The availability of data for each of these locations, as well as their positioning on the ACP, makes them ideal for this study.

This study was designed to examine lakes expansion at multiple spatial and temporal scales to better understand lakeshore expansion. By looking at differences in expansion rates between lake regions, differences between lakes within a region, and differences within a single lake, my goal was to establish the dominant driving and resisting factors behind lakeshore erosion on the ACP. After choosing the study regions and selecting lakes, the first step of analysis was to establish lakeshore expansion rates among lakes within the three different regions, YOCP, OCP, and ICP. These regions were chosen to cover a variety of landscape types and conditions on the ACP, while maintaining the similar features of high lake density of approximately 20% (Hinkel et al., 2005) and climate conditions.

Lakes were chosen within each study region for a variety of reasons. First, lakes that had ongoing measurements were chosen from each study area. Other lakes within each study area were chosen based on the availability of historical imagery and other characteristics that would make them favorable for this study, including size distribution and ice regime. These chosen lakes were compared initially strictly by region, to see what region scale factors effect these processes.

To better understand the differences between lakes within a region, these lakes were examined by their size and other lake specific factors. One of the main differences, and one readily observable through remote sensing, was that of ice regime. By looking at a lakes ice regime with Synthetic Aperture Radar (SAR) imagery, I compared whether lake ice had frozen to the bed of a lake by the end of winter or if there was still liquid water beneath the ice. Whole lakes were classified as either bedfast or floating ice, and for a subset of 6 lakes, floating ice lakes were classified as having either bedfast or floating ice conditions within 100 m of shore.

To better understand the heterogeneity of expansion rates around the perimeter of a single lake, the landscape around each of 6 lakes within the YOCP was broken out into three distinct terrain units to determine the relative expansion rates for each. The original terrain unit map (Lara, unpublished) was simplified into 3 distinct terrain units for the region by combining with a 5m IFSAR digital elevation model to weight lake bluff height. This produced a map showing three distinct terrain units classified as the primary surface (PS) unit, the flat centered polygon (FC) unit, and the low centered polygon (LC) unit.

Table 2: Pertinent characteristics of each lake examined in this study, including region, ice regime, lake area, lake elevation, lake orientation, and dominant terrain unit.

Region/Lake	Regime	Size (ha)	Elevation (masl)	Orientation (°NNW)
YOCP				
Tes001	Floating	1025	3.6	20
TesB	Bedfast	148	3.7	9.6
TesF	Floating	23.5	2.5	107.4
Specklebelly	Floating	284	0.6	14.6
Tes2	Bedfast	284	2.5	9.4
Peatball	Floating	117	3.8	17.2
Wadepiper	Bedfast	36.6	3.9	8.1
TesH	Bedfast	451	1.4	16.1
TesI	Bedfast	372	0.6	3.2
TesJ	Floating	418	2.5	15.1
TesK	Floating	251	2.8	9.8
TesL	Bedfast	381	0.7	10.4
TesM	Floating	296	1.5	12.5
TesN	Bedfast	149	3.8	6.4
TesO	Bedfast	112	3.7	13.1
Wtwin	Floating	123	2.0	5.2
Etwin	Bedfast	128	1.6	9.5
OCP				
B100	Floating	184	7.9	6.4
BRWA	Floating	94	9.0	12.8
BRWC	Floating	115	1.0	6.2
BRWB	Bedfast	71	3.6	6
BRWE	Floating	437	5.2	14.1
BRWF	Floating	246	2.2	12.7
Pingoakeok	Floating	304	8.3	18.2
ICP				
FCWC	Bedfast	50.4	4.6	26.5
FCWD	Floating	135	15.4	24.2
FCWE	Floating	227	20.3	21.7
ITIL22	Floating	300	26.3	23.5
ITIL27	Floating	154	24.6	15.8
ITIL50	Floating	12.0	8.9	11.1
L919	Floating	107	6.8	20.9
R0066	Floating	101	22.0	11.2
L9811	Floating	419	18.9	3.9
M9925	Bedfast	87.3	13.0	38.2
MC7916	Floating	168	0.5	115.1

3. Methods

3.1 Image Acquisition and Processing

Aerial photography scenes acquired at 1:20000 scale from the summers of 1948 and 1949 from the Barrow Arctic Research (BAR) Lab were georeferenced to a 2.5 m color infrared orthophoto mosaic acquired in 2002 (Table 3). For a subset of lakes within the YOCP, additional CIR aerial scenes were acquired from the summer of 1979. These images were acquired through USGS Earth Explorer, part of the Earth Resources Observation Science (EROS) Center. Imagery was georeferenced with ground control points (GCP) to distinct features that remained stable over the study period and to a spatial resolution of 0.5 m. Typically, GCPs were ice wedge polygon intersections and small islands in inundated lowland areas. Each scene required an average of 15 GCPs to accurately georeference using a 3rd order polynomial transformation to achieve mean RMS error of under 1m per scene. Average RMSE across all lakes was 0.45 m (sub-pixel). Lake shorelines for the 1948 BAR imagery, 1979 CIR photos, and 2002 CIR orthomosaic were manually delineated (Figure 3a).

Table 3: Summary of imagery used for delineation of lake shorelines (1948, 1979, 2002) and lake ice regime characteristics (2016). Aerial photography was acquired through USGS Earth Observation Science Center's EarthExplorer page, and the SAR imagery was collected by the European Space Agency and acquired through the Alaska Satellite Facility.

Time of Acquisition	Type	Source	Scale	Pixel Size (m)
July/August 1948/1949	Black and White Aerial Photography	USGS EROS	1:20000	0.5
1979	Color Infrared Aerial Photography	USGS EROS	1:63000	2.5
July/August 2002	Color Infrared Aerial Photography	USGS EROS	1:40000	2.5
April 2016	Sentinel-1 C band SAR	European Space Agency	-	10

Dilution of Accuracy (DOA) calculations were made following Jones, 2009 and modified from Hapke (2005) and Lantuit and Pollard (2008) using Equation 1:

$$\boldsymbol{DOA} = \frac{\sqrt{(E_g)^2+(E_{p1})^2+(E_{p2})^2+(RMS_1)^2+(RMS_2)^2}}{\Delta T} \qquad \textbf{(1)}$$

Where E_g is the positional accuracy of the 2002 CIR orthomosaic (determined to be ±5 m), E_{pn} is the pixel resolution for the imagery from each year, RMS_n are the root mean square errors of the georegistration process, and ΔT is the time interval between the given data sets. Using this formula, the 1948 images were georeferenced to the 2002 orthomosaic with an average DOA of 0.10 m/yr. The average DOA for the 1948 to 1979 datasets was 0.27 m/yr and the DOA for the

1979 to 2002 datasets was 0.19 m/yr. These values represent the minimum detectable erosion rate between each time period.

3.2 Shoreline Change Detection

To calculate expansion rates around the lake perimeter, I used the Digital Shoreline Analysis System (DSAS) tool (Thieler *et al*., 2005). Transects were cast every 25-50 m, depending on lake size, orthogonal to the modern shoreline of the lake and the average rate was calculated between the two shoreline intersections (Figure 3b). The per-transect rates were used to average whole lake expansion rates for each lake in the study. For a subset of 6 lakes within the YOCP, an additional dataset of 1979 acquired CIR aerial scenes (Table 3) was also georeferenced and shorelines manually digitized. For this subset of lakes, average expansion rates from 1948 to 1979 and average rates from 1979 to 2002 were calculated.

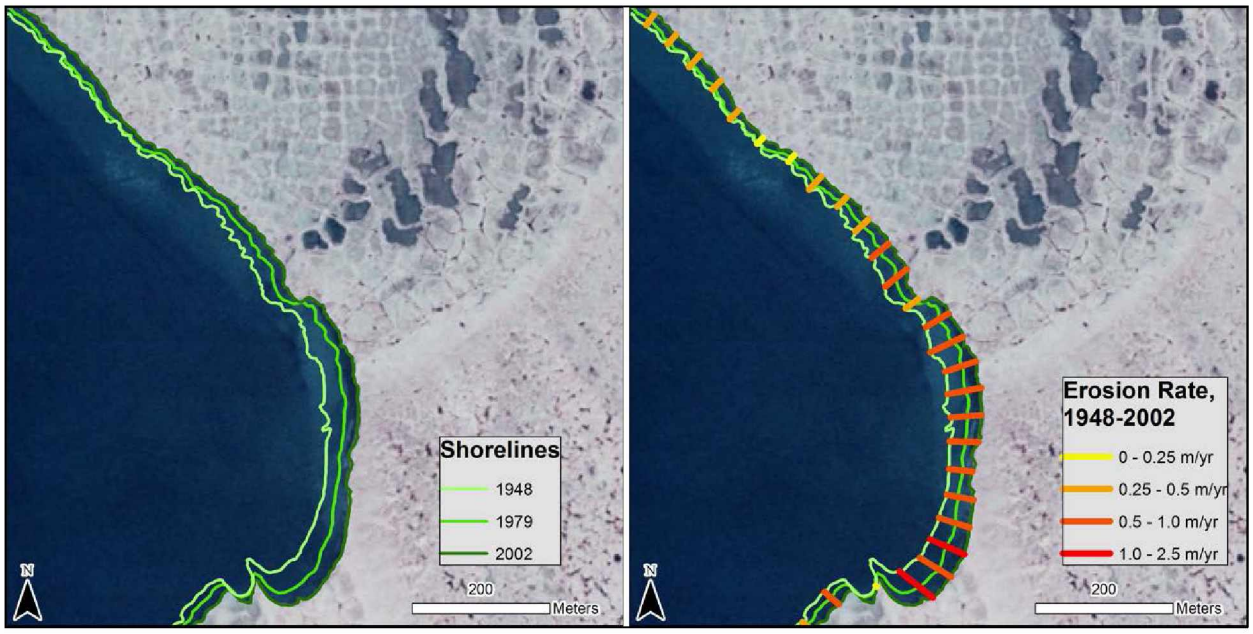

Figure 3: Example of shoreline delineation (a) and DSAS transect casts (b). Base imagery is 2002 CIR, with 1948, 1979, and 2002 shorelines traced in green. Transects in (b) are clipped to shoreline change envelope and colored according to average erosion rate over the period 1948-2002.

3.3 Ice Regime Analysis

To determine the ice regime of a lake, I relied on both field measurements and analysis of synthetic aperture radar imagery. Specifically, I used a 10 m Sentinel 1A C-band ESA satellite image acquired on April 20, 2016 VV polarization. Using knowledge of radar return differences between bedfast ice and floating ice lakes, lakes that were greater than 75% bedfast were given the bedfast designation, and lakes greater than 25% floating were given the floating ice designation. Typically, a bedfast ice lake will be all bedfast with no remaining pockets of liquid water, but a floating ice lake may have significant portions of their area with bedfast ice. Where floating ice lakes will appear as bright areas in the radar image, bedfast ice lakes will have a lower backscatter return and will therefore appear dark. For a subset of 6 floating ice lakes within the YOCP, nearshore ice conditions were also determined to analyze the relative expansion rates of lake in an area with nearshore bedfast ice conditions compared to nearshore floating ice conditions.

To estimate bedfast and floating ice conditions within 100 m of modern shorelines, I used the same Sentinel 1A SAR imagery in conjunction with the product of the DSAS protocol in section 4.1. Training polygons were established within regions known to experience either bedfast or floating ice conditions, and a maximum likelihood classification was performed using these training polygons. In this way, the entire acquisition area was classified according to bedfast or floating ice conditions. This output data was smoothed with an 8 neighbor majority filter. Using shorelines digitized from 2002 CIR imagery, a buffer was created stretching 100 m offshore of modern shorelines and the classified raster was clipped to the extent of these buffers for 6 floating ice lakes; 3 in the YOCP and 3 on the OCP Peninsula. Within these buffers, statistics were calculated for each transect. I calculated the percentage of the intersecting shoreline that was

classified as bedfast or floating, classifying areas with 50% or greater bedfast pixels as a bedfast shoreline, and areas with fewer than 50% bedfast pixels as a floating ice shoreline.

3.4 Terrain Unit Analysis

To analyze the control that the terrain unit of the corresponding shore exerts on expansion rates, I analyzed the terrain units within the YOCP region using a combination of techniques. The ACP terrain unit map from (Lara, In Press) was combined with the 5 m IFSAR DEM, and then classified according to terrain unit and elevation. The resulting classification yielded three classes apart from open water (Figure 4). The first, called the primary surface (PS) unit (O'Sullivan, 1961; Brown, 1965), is the highest elevation surfaces within the YOCP. Composed primarily of late stage high center polygons, these areas are considered to be the oldest surfaces within the study area and have not been previously reworked by lakes. Ice wedge networks within the PS are mature, with wide and deep ice wedges and strong segmentation of ice wedge polygons (Leffingwell, 1915) (Figure 5). Each of the other terrain units is the remnant of a lake basin that has drained in the past and begun to recover through time. The first is composed of flat centered polygons and dry low centered polygons, and for simplicity is referred to as flat centered (FC). This unit displays segmentation of polygons and is typically situated slightly above lake level (Figure 5), though without the tall bluffs one might see for the PS unit. The final unit is characterized by inundated low center polygons and is referred to as LC. Segmentation in this unit is weak, meaning relatively small ice wedges compared to the other units, and these areas are typically very near to lake surface elevation (Figure 5). This is likely the youngest surface between these three.

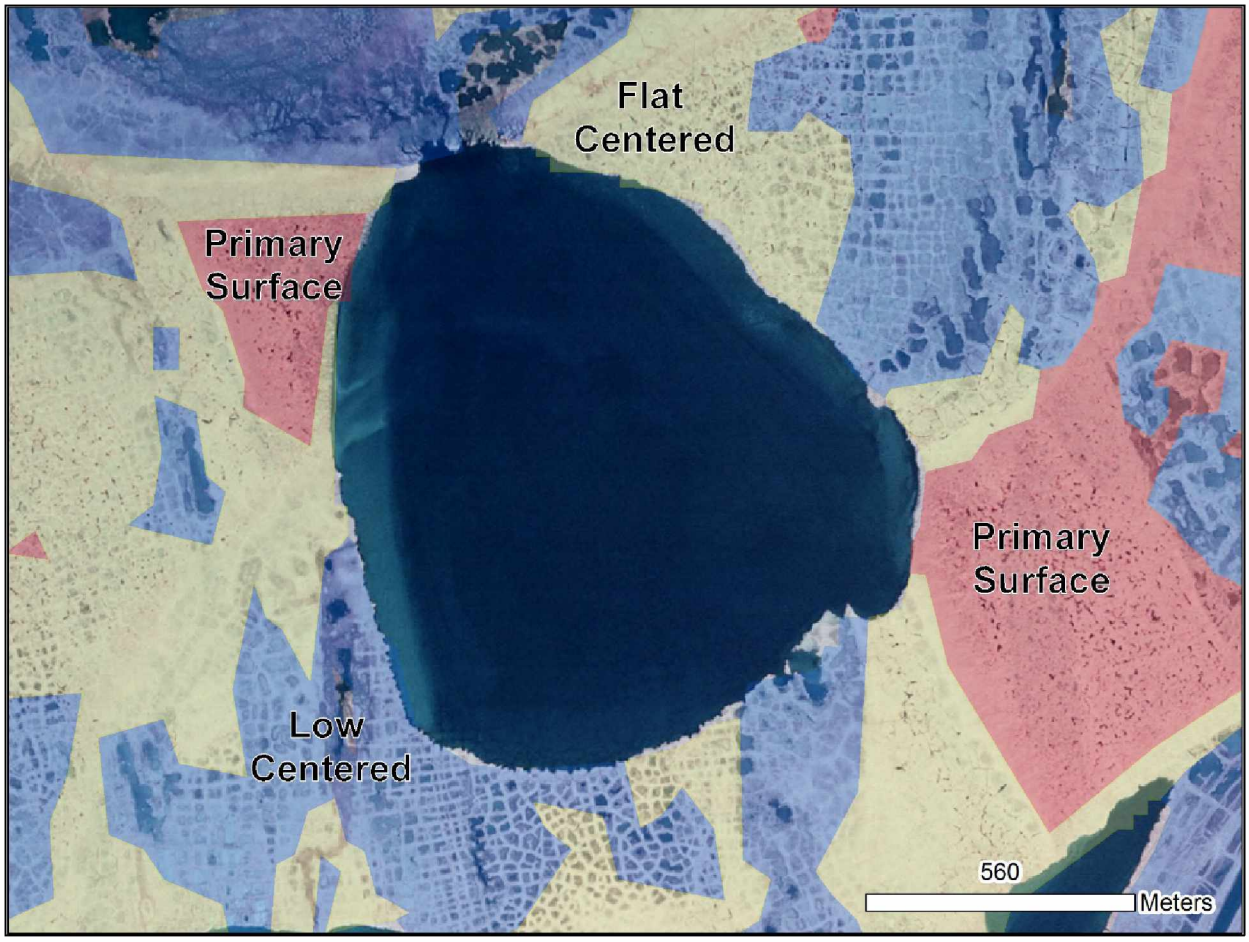

Figure 4: Showing the results of terrain unit classification on Peatball Lake. Primary surface units are delineated in red, flat centered polygons are delineated in yellow, and low centered and inundated polygons are delineated in blue.

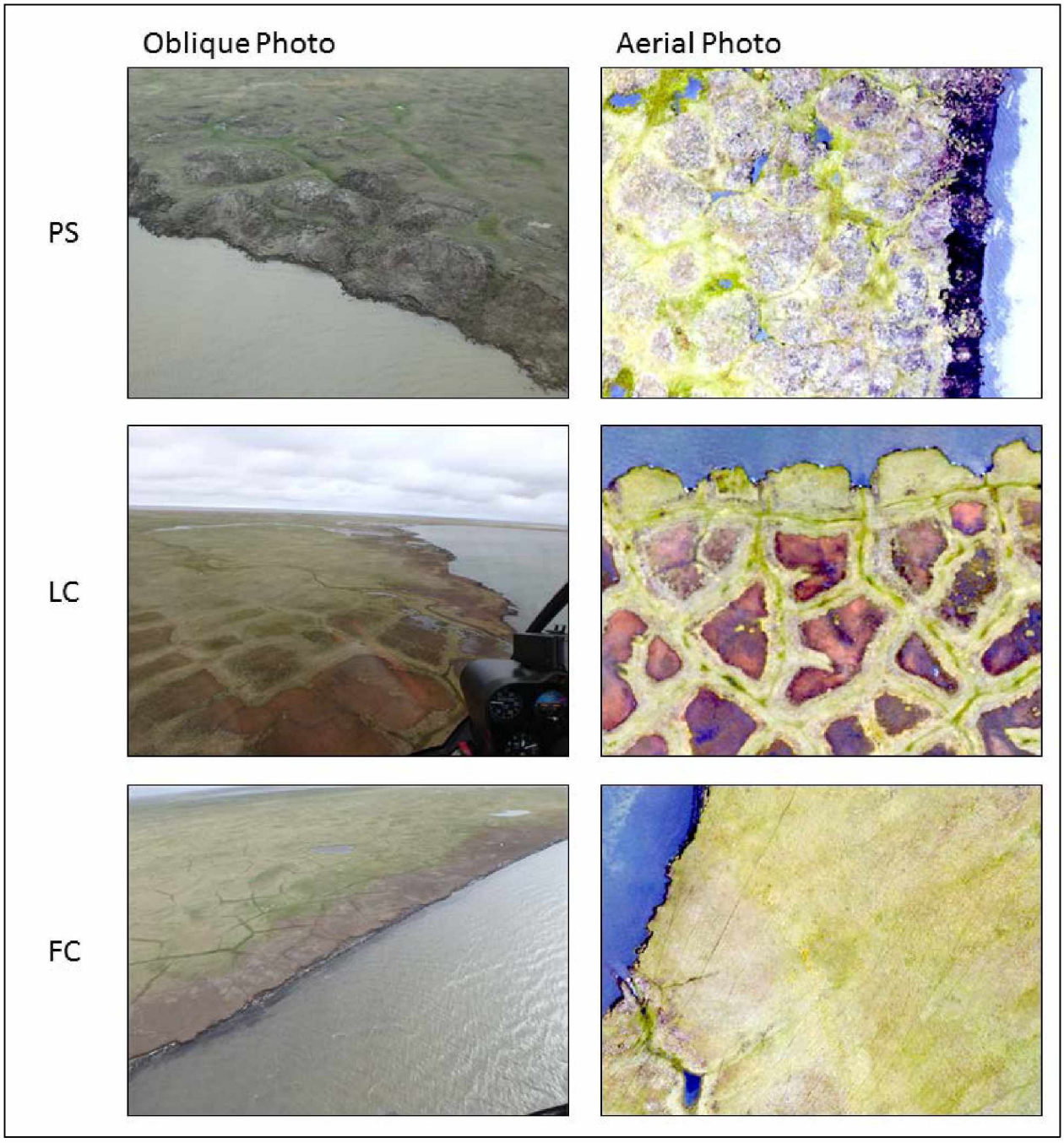

Figure 5: Examples of terrain units extracted from terrain unit analysis. All units are shown first in oblique view from helicopter, and second in orthorectified aerial photos acquired in August of 2015.

3.5 Field Verification and Shoreline Characterization

Field work was conducted throughout the YOCP and to a lesser extent in the ICP and OCP to directly observe the characteristics of lakeshore expansion and how they relate to winter time processes, summer thaw, and terrain unit properties. In late summer of 2015, I measured active layer depths at a number of transects within the YOCP orthogonal to shorelines, starting in undisturbed tundra and continuing into the shallow littoral area of the lake. Care was taken to include a variety of shoreline types, from low flat shorelines to tall lake bluffs, around the entire perimeter of the lake as time allowed. I used 16 mm steel rods with a tile probe tip with total length of up to 3.2 m. Shallow active layer depths were driven by hand, but deeper thaw depths required the use of a slide hammer until the probe met refusal. In situations where thaw depth was greater than length of probe, the thaw depth was recorded as greater than 320 cm. Active layer depths were evaluated as a proxy for ground thermal state and for their relationship to shoreline type, lake ice regime, and relative lakeshore expansion rates.

During this same field season, I installed thermistors along a number of these transects. HOBO U23-003 Pro v2 temperature loggers were installed at 0.5 m and 1.0 m depth below ground surface in 4 locations per transect; upland tundra, upper shoreline, lower shoreline, and shallow littoral. Loggers recorded temperatures at 1 hour intervals for one full year, and were retrieved the following summer in 2016. Partly due to the extreme climate conditions of the North Slope of Alaska and their location on an actively eroding lake shoreline, many thermistors did not survive through until the next field season.

To determine representative characteristics of terrain units identified in remote sensing analysis, I took a series of 3 cores in 3 different DTLBS in the YOCP. I used a 5 cm diameter SIPRE barrel to core sites near shorelines, taking care to avoid ice wedges. Cores reached an

average depth of 2.5 m. Because the relative elevations of the primary surfaces often precludes coring to depths equal to the lake surface elevation, details on this unit were established during summer months at exposures at lake shores. I sampled them by scraping away the thawed material to expose frozen surfaces. I took samples with battery powered hand drills equipped with a hole saw from each horizon for testing. Rough vegetation information was also recorded, along with photographs, for further identification of units. Core samples and samples taken from lake bluff exposures were transported and stored frozen until such time they could be subsampled. Cores were sampled with 10cm long core sections taken at every 25cm interval. These subsamples along with all samples taken from lake bluff exposures were weighed in their frozen state, dried at 90 °C for 72 hours, and weighed again to calculate gravimetric moisture contents for each site (Equation 2).

$$\boldsymbol{GMC}(\%) = \frac{\boldsymbol{m_{water}}}{\boldsymbol{m_{dry\ soil}}} = \frac{\boldsymbol{m_{wet\ soil} - m_{dry\ soil}}}{\boldsymbol{m_{dry\ soil}}} \boldsymbol{x100} \qquad \textbf{(2)}$$

where GMC is the gravimetric moisture content, $m_{wet\ soil}$ is the mass of soil and ice together, and $m_{dry\ soil}$ is the mass of soil only after drying.

In April of 2016, a series of snow survey transects were also conducted around the perimeter of 8 lakes. Two side-by-side transects were performed at each of the cardinal directions around the lake. Snow depths and positions were measured with a GPS Snow Depth Probe (Magnaprobe, Snow-Hydro, Fairbanks, AK, USA) and with a graduated avalanche probe. These transects were performed orthogonal to shoreline, starting in an upland tundra location where snow drifting appeared to be unaffected by the bluff height and stretching to approximately 50-100 m onto the lake (ice) surface where snow drifting appeared unaffected by the bluff height. Snow depths were examined for trends related to shoreline type, distance from shore, and relationship to

lakeshore expansion rates in order to better understand the role that drifting snow plays in the shoreline erosion processes that control lakeshore expansion.

During July of 2016, I visited 6 lakes within the YOCP region and 2 within the ICP region for the purpose of shoreline characterization. Through on the ground investigation and by circling the shoreline from helicopter, I was able to qualitatively characterize some representative shoreline types for the mechanism of shoreline erosion relative to factors such as bluff height and terrain unit, lake ice regime, and local geology and document these processes through field photographs. This data was used to establish which, if any, processes of shoreline erosion were responsible for increased expansion rates relative to others.

4. Results

4.1 Regional Scale Thermokarst Lake Expansion Rates

Average expansion rates varied considerably between the three study areas between 1948 and 2002 (Figure 6 and 7). For the period of 1948 to 2002, the highest overall expansion rates were observed in the YOCP, with a mean of 0.62 m/yr (n=17). The OCP had the second highest expansion rates with a mean of 0.57 m/yr (n=7) and the ICP had the lowest average expansion rates of 0.16 m/yr (n=11). Despite having the highest average expansion rates overall, the YOCP had the greatest variability in expansion rates as well, with a standard deviation of 0.51 m/yr. In fact, two lakes within the YOCP (Wadepiper, rate = 0.06 m/yr and TesN, rate = 0.17 m/yr) had lower expansion rates than the lowest rate found in OCP (BRWB, rate = 0.22 m/yr) and the average expansion rate for ICP (0.16 m/yr). Overall, the OCP was much more consistent in its expansion rates with a standard deviation of 0.28 m/yr. The ICP had the lowest standard deviation of all regions studied, of 0.14 m/yr, but still had lakes that ranged from an average rates as high as 0.5m/yr to as low as 0.05 m/yr or below the detection limit of the dataset. The YOCP is the most dynamic region studied, having both the highest and very close to the lowest rates of erosion observed in this study, with rates distributed fairly evenly between these two extremes. The lakes in this region also tend to be more variable in size and landscape setting than in either of the other two regions.

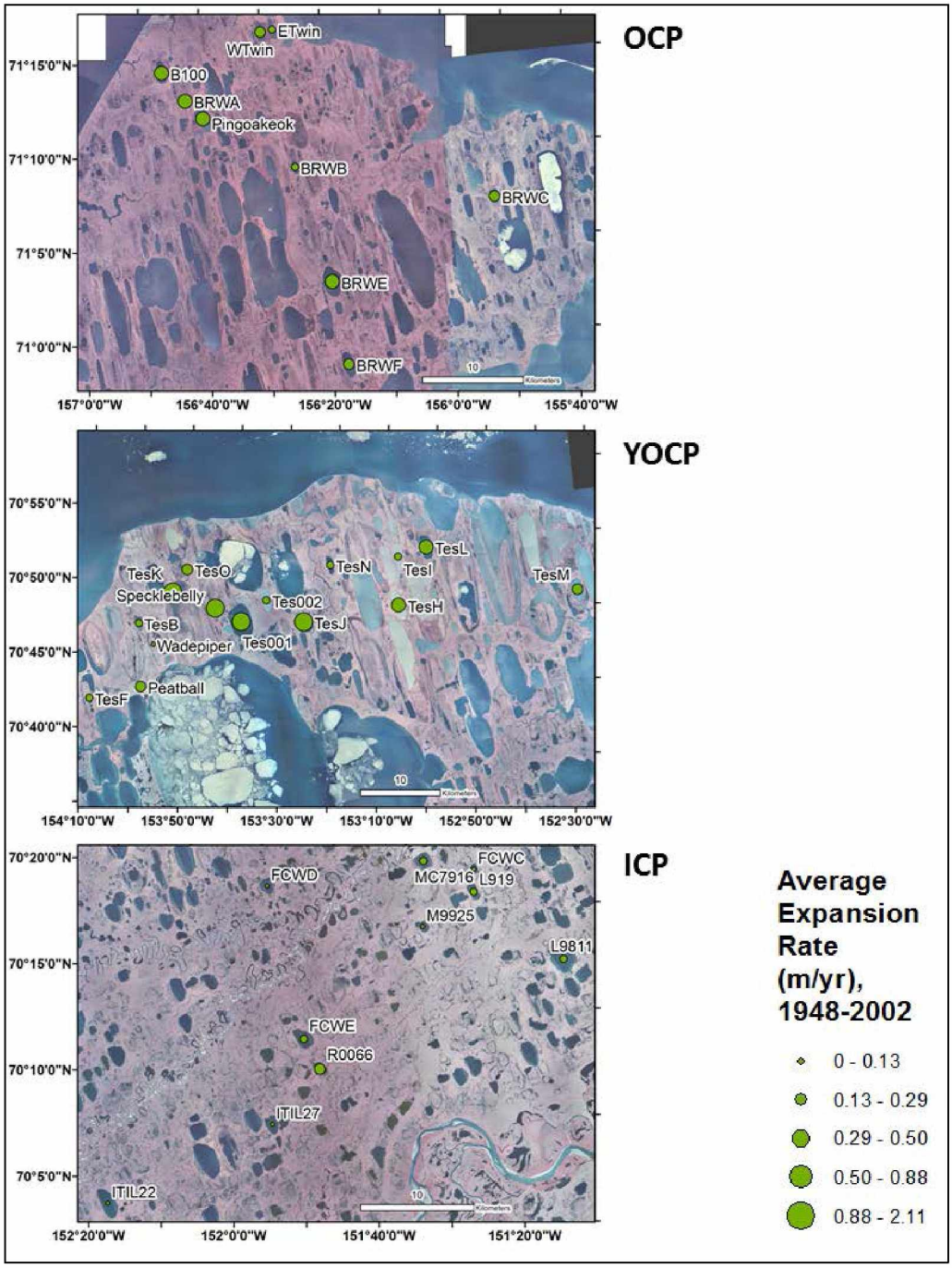

Figure 6: All lakes within the study are plotted on 2002 CIR imagery, divided by region. Point size correlates to average yearly expansion rate for the time period 1948-2002.

Table 4: All lakes analyzed in this study, divided by region and ice regime. Average expansion rates 1948-2002 and size increase, both in hectares and percentage, are presented.

Region / Lake	Regime	Rate (m/yr)	% size increase
YOCP			
Tes001	Floating	1.29	8.8
TesB	Bedfast	0.29	4.9
TesF	Floating	0.27	10.7
Specklebelly	Floating	1.29	18
Tes2	Bedfast	0.26	3.3
Peatball	Floating	0.48	9
Wadepiper	Bedfast	0.06	2
TesH	Bedfast	0.82	10.6
TesI	Bedfast	0.2	1.7
TesJ	Floating	1.36	14.8
TesK	Floating	2.11	39.1
TesL	Bedfast	0.6	6.7
TesM	Floating	0.37	4.5
TesN	Bedfast	0.17	3.7
Etwin	Bedfast	0.27	5.9
Wtwin	Floating	0.38	7.5
TesO	Bedfast	0.4	7.9
OCP			
B100	Floating	0.88	15.8
BRWA	Floating	0.65	13.6
BRWC	Floating	0.44	8.9
BRWB	Bedfast	0.22	5.9
BRWE	Floating	0.64	7.2
BRWF	Floating	0.39	4.9
Pingoakeok	Floating	0.79	10.3
ICP			
ICPC	Bedfast	0.13	3.8
ICPD	Floating	0.09	1.5
ICPE	Floating	0.19	2.6
ITIL22	Floating	0	0
ITIL27	Floating	0.09	1.5
ITIL50	Floating	0.03	1.3
L919	Floating	0.25	5.9
R0066	Floating	0.5	10.6

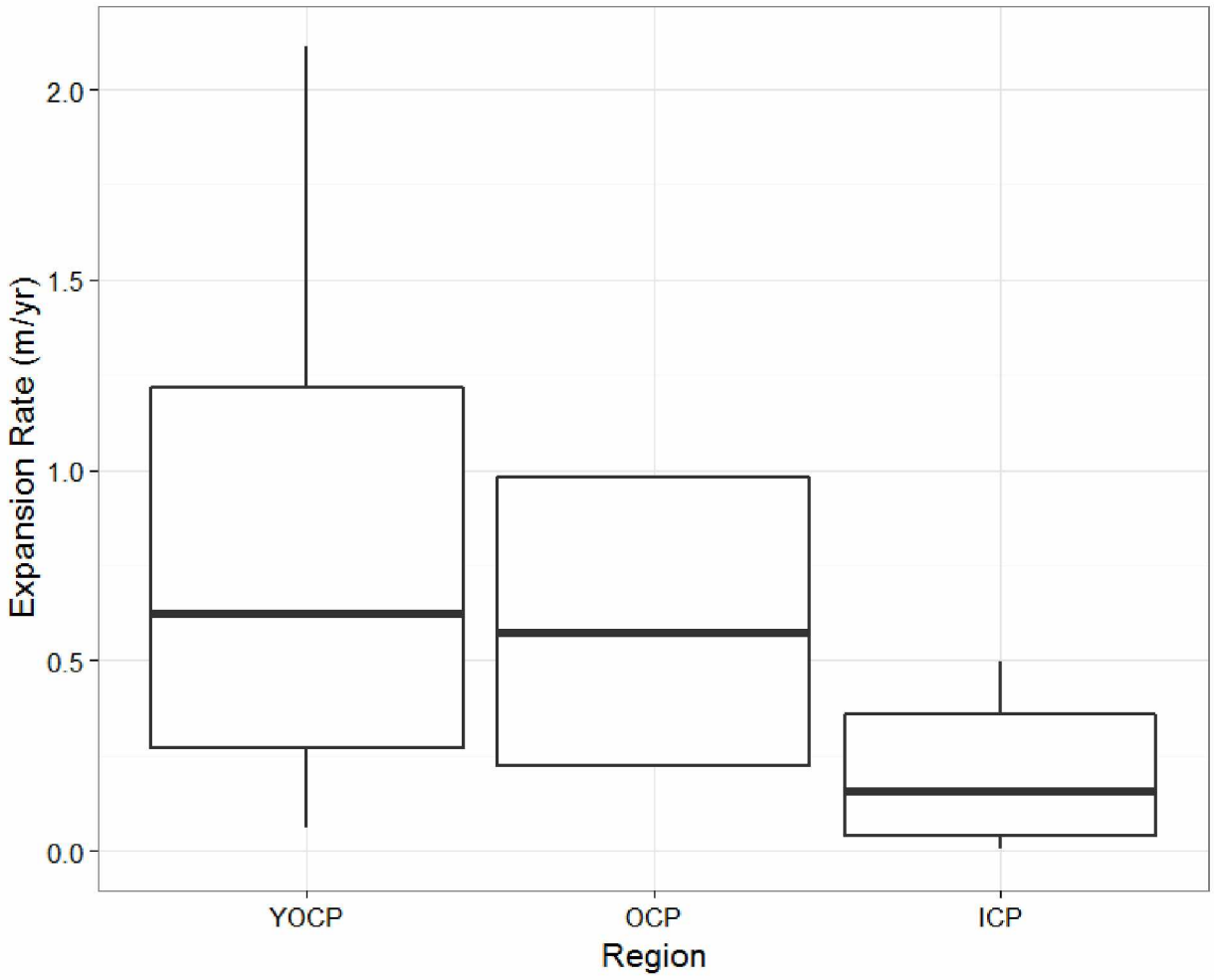

Figure 7: Mean expansion rates of all lakes within each region showing high expansion rates in YOCP, slightly lower in the OCP region, and low overall rates of lakeshore expansion in ICP. Boxes represent 10th and 90th percentile.

Another key difference is the size distribution. Lakes within the YOCP generally have a much broader size distribution than lakes within the other regions. Most of the largest lakes studied are within the YOCP, with some greater than 1000 ha in area. Average lake size among those studied for the YOCP was 321 ha, while average lake size for OCP was 170 ha and 160 ha for

ICP. YOCP had the largest variation in size, with the smallest lake at 23 ha and largest was 1025 ha with an overall standard deviation of 278 ha. ICP had a standard deviation of 117 ha, and OCP a standard deviation of 91 ha. The smallest lake of the study set was within the ICP, at an area of 12ha. This underscores the fact that lakes in the OCP and ICP are both relatively homogenous in respect to lake size, each having a standard deviation of less than half that of the lakes within the YOCP.

Among all lakes in all regions studied, average erosion rates increased with lake area (Figure 8). This pattern was consistent in both the YOCP and OCP regions, but lakes within the ICP did not show this pattern as strongly and are in fact expanding at a slower rate on average. The pattern of increasing expansion rates with lake area was more pronounced once rates exceeded approximately 0.5 m/yr on average in lakes larger than 100 ha (Figure 7). The largest lake where I measured erosion, Tes-001 (1025 ha), located in the YOCP, deviated from this pattern with an average erosion rate, 1.29 m/y, similar to several smaller lakes, 283 ha and 417 ha , with average erosion rates ranging from 1.29 to 1.36 m/yr (Figure 6, Tables 2 and 4). At a landscape scale, the fast erosion rates of larger lakes leads to a widespread transformation of tundra land area to lake area. In some cases, lakes experience a 10% or greater increase in area over the period 1948 to 2002. On the largest lakes surveyed, this can be an increase of over 100 ha in lake area.

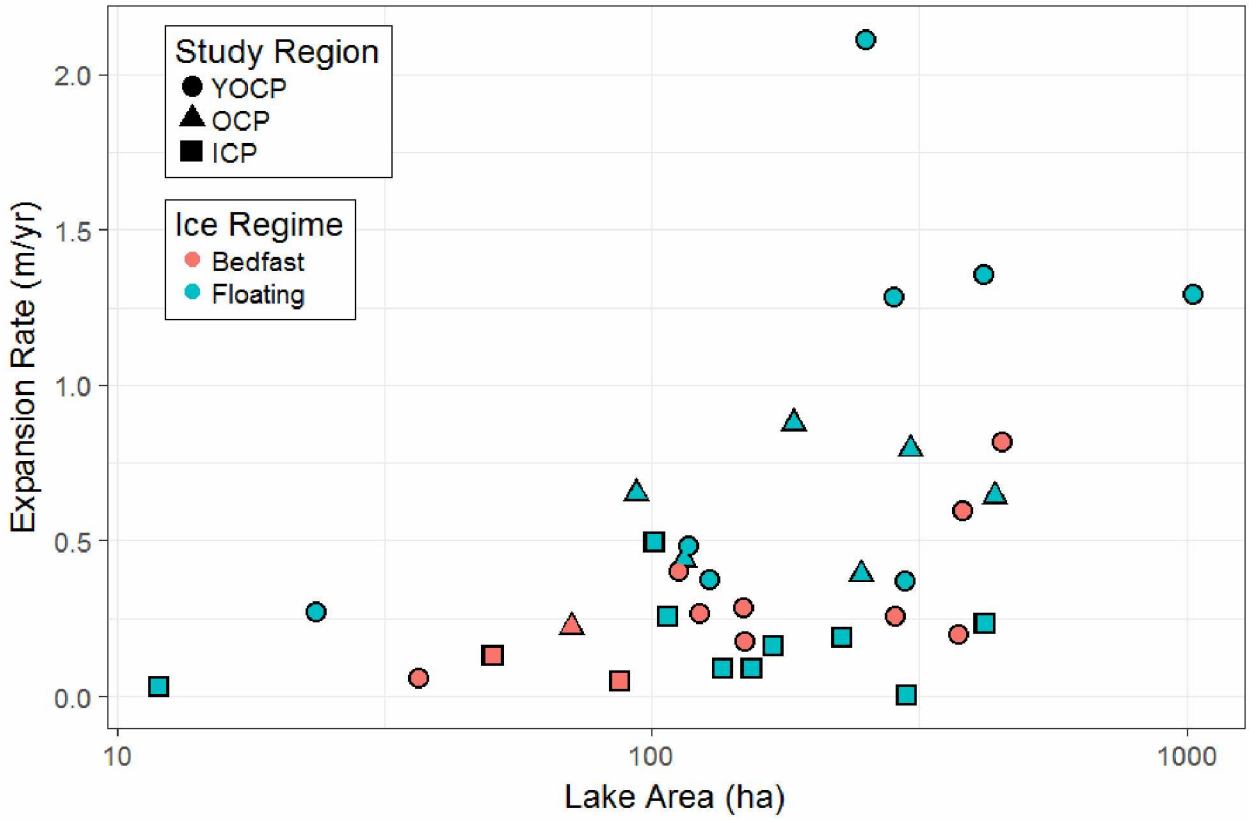

Figure 8: Comparison of shoreline erosion rates (averaged from 1948-2002) to lake area for the YOCP, OCP, and ICP study areas in northern Arctic Coastal Plain of Alaska.

4.2 Impact of Ice Regime on Thermokarst Lake Expansion

When lake expansion rates are compared on the basis of their late winter ice conditions, an important pattern emerges. Lakes that experience floating ice conditions over 75% of their surface area had an average expansion rate of 0.47 m/yr over the period of 1948 to 2002, compared to bedfast ice lakes which had an average expansion rate of only 0.30 m/yr. Even though the magnitudes vary in the study areas, the relative difference is evident across all study areas (Figure 9). OCP bedfast lakes expand at 0.3 m/yr relative to floating ice lakes that expand at 0.6 m/yr, whereas YOCP bedfast lakes expanding at 0.37m/yr vs floating ice lakes expanding at 0.94 m/yr,

and ICP bedfast lakes expanding at 0.09 m/yr compared to floating ice lakes expanding at 0.17 m/yr. The greater the average expansion rate for a region, the greater the difference was between rates for the two ice regimes, with YOCP having the greatest difference between bedfast and floating ice lakes, and ICP having the smallest difference between them. For every region, however, the maximum expansion rate for any bedfast lake is still higher than the minimum expansion rate for any floating ice lake within that region. Floating ice lakes in general experienced greater variability in expansion rates than their bedfast counterparts. When normalized by average rate, the standard deviation for floating ice lakes was 0.95 compared to a value 0.76 for bedfast ice lakes after the same normalization.

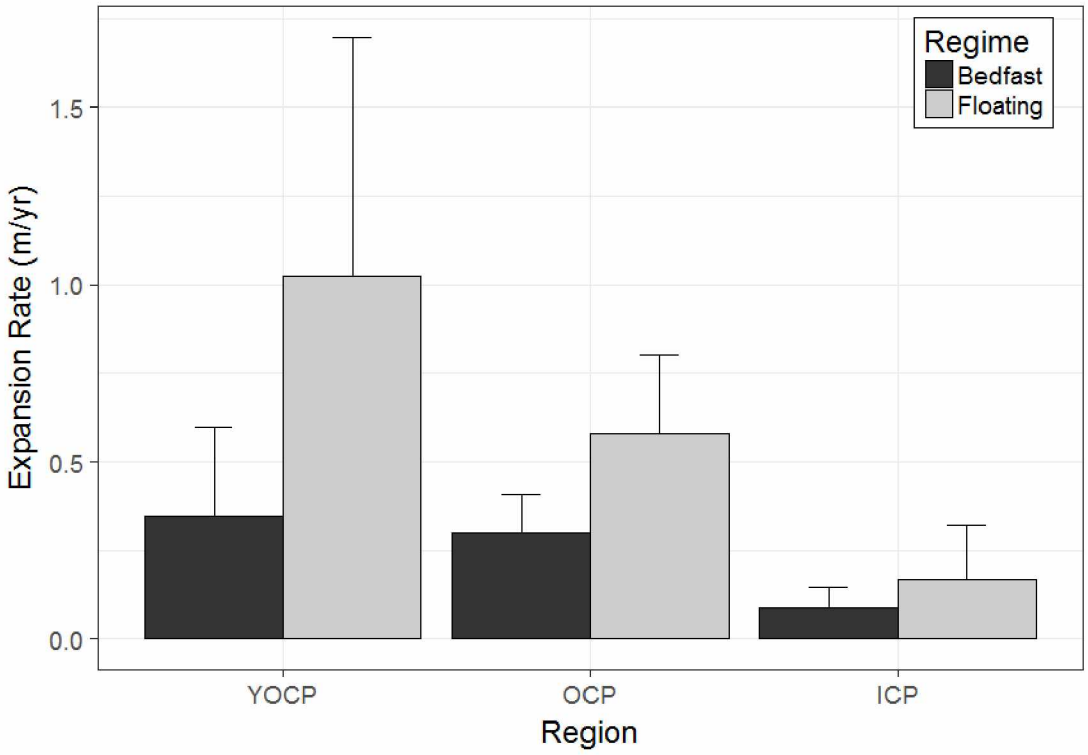

Figure 9: Average lakeshore expansion rates for the period 1948-2002 for three regions on the ACP, showing differences between bedfast and floating ice regimes consistent across all study regions. Error bars are S.D. for each data set.

This pattern of bedfast ice conditions exerting strong controls on lakeshore expansion rates is consistent in the nearshore conditions (within 100 m of shore) for floating ice lakes. Where lakes have a shallow shelf that experiences bedfast conditions in late winter, expansion rates are significantly slowed compared to areas of the lake which experience primarily floating ice conditions. For an intensive subset of floating ice lakes within the YOCP and OCP, expansion rates along shorelines that experience bedfast ice conditions were 0.32 m/yr compared to 0.85 m/yr for areas with predominantly floating ice conditions within 100m of shore (Figure 12). When normalized for whole lake expansion rates, the pattern was consistent across most of the lakes in the study. The two exceptions to this were Peatball Lake and West Twin Lake in the YOCP region. West Twin's rates were very similar in both the bedfast and floating ice regions of shore, and saw little deviation from the whole lake rate observed. Both of these lakes have relatively low whole lake expansion rates. Among lakes which showed higher expansion rates along their floating ice shorelines compared to the bedfast shorelines, there was some variation in the relative differences between ice regimes, but overall the same pattern was observed. Where floating ice shorelines showed a substantial increase in expansion rate over bedfast shorelines, specifically for lake B100 (bedfast shores rate = 0.41 m/yr, floating ice shores rate = 0.95 m/yr), it should be noted that this is within a different region (OCP) than the other lakes observed to follow the pattern. Within the YOCP, patterns were relatively stable, and showed an approximate 50% increase in expansion rates over the bedfast ice shorelines. For lakes with higher whole lake expansion rates, like Tes001 (rate = 1.29 m/yr), Specklebelly (rate = 1.29 m/yr), and even B100 (rate = 0.88 m/yr) the differences between the two shoreline types were more pronounced. Lakes that had lower overall expansion rates saw smaller differences between the two shoreline types, or even a reversal of the average pattern.

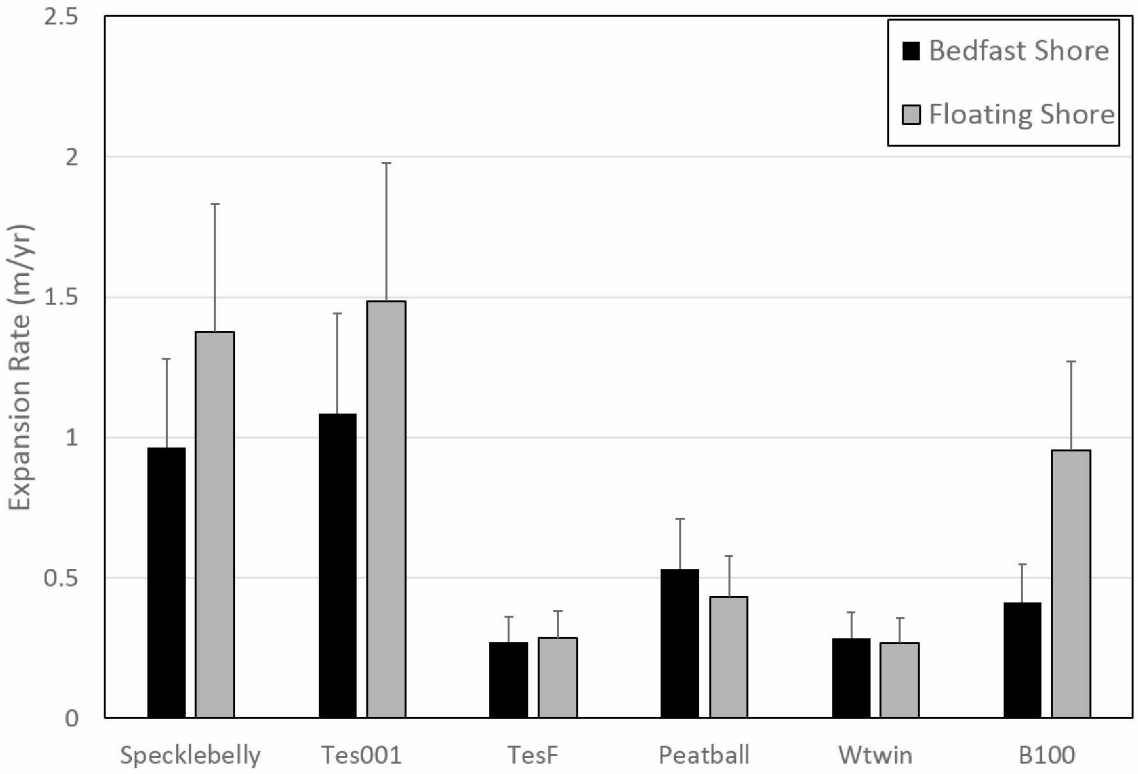

Figure 10: Examples from 6 floating ice lakes in the YOCP and OCP regions of differential expansion rates depending on bedfast vs floating ice regime within 100m of shore as determined through the use of late season C-band satellite imagery. Expansion rates are averaged over the period 1948-2002, error bars represent S.D.

4.3 Thermokarst Lake Orientation

The analysis of all transects across lake shorelines demonstrate that lakes in general are expanding fastest at their northern and southern ends. This varies considerably across study areas and between lake types, though. ICP for instance shows little to no pattern in regards to expansion direction, for either bedfast or floating ice lakes. OCP, where lake orientation is already the strongest, is where we begin to see some of this oriented expansion at the northern ends of lakes, particularly on bedfast ice lakes within the region. Between 315°-360°, expansion rates are greater than in any other direction, and are nearly twice as high as whole lake expansion rates for bedfast ice lakes in OCP. Interestingly, this is the same general direction as the long axis of the oriented lakes in this region (332°). The floating ice lakes in this region do not show the same expansion pattern, with rates nearly uniform in all directions (Figure 11).

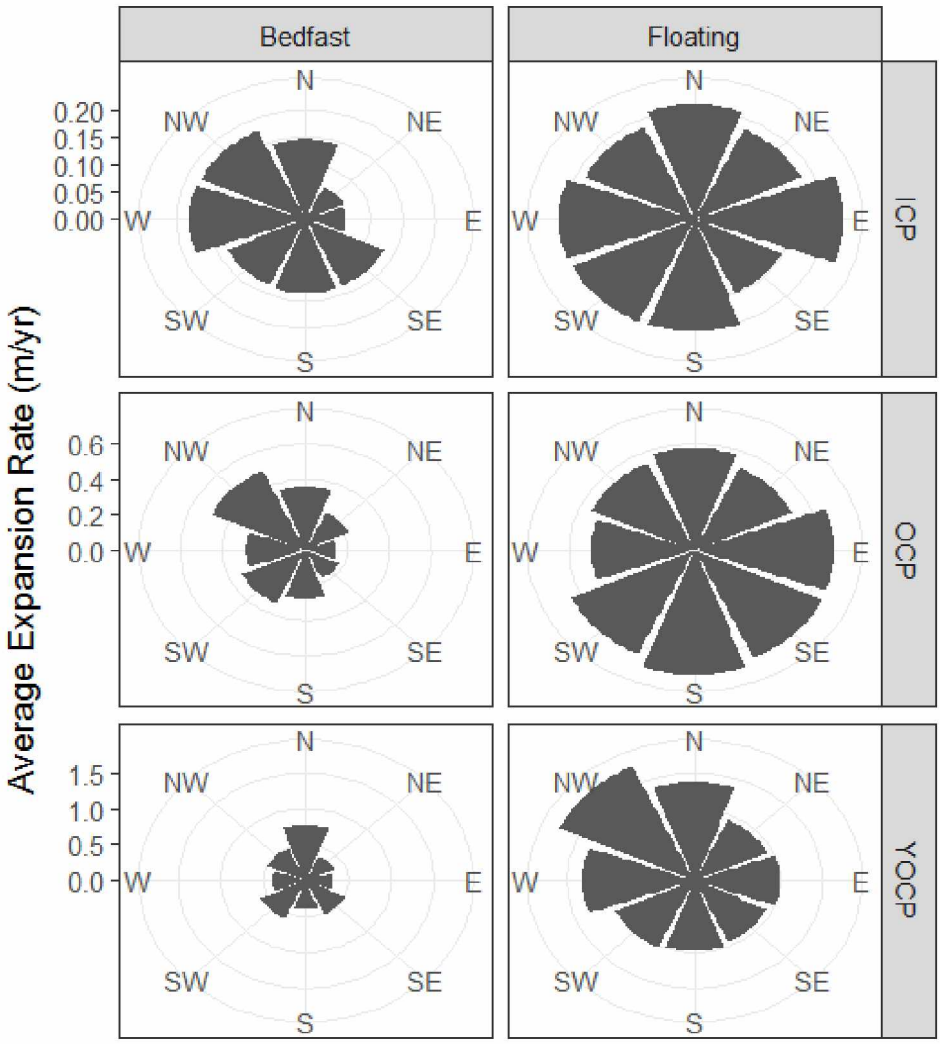

Figure 11: A presentation of the mean erosion directions for bedfast ice and floating ice lakes in each study region. Bedfast lakes in the OCP and YOCP regions and floating ice lakes in the YOCP show a pattern of oriented expansion in the N-S direction.

YOCP is the region with the strongest pattern of lakes showing oriented expansion, and this occurs in both floating ice and bedfast ice lakes. For the bedfast ice lakes, expansion is greatest between 0°-45°, at greater than twice the average whole lake expansion rates for bedfast ice lakes in the YOCP. There is also a significant increase in rates in the northwest & south/southwest region of lakes, where expansion on the eastern and western shorelines on lakes were lower than

whole lake averages (Figure 12). What is interesting about the YOCP specifically is that the floating ice lakes show a strong pattern of erosion, with average rates of nearly 1.5 m/yr in the region between 315°-360°, much higher than the average of 0.94 m/yr for floating ice lakes in general. This too aligns with the long axis of oriented lakes on the ACP, and although lakes in the YOCP have a smaller length to width ratio than lakes (1.9) in the OCP region (2.1), the lakes in the YOCP do tend to have a long axis oriented at an average of 342°, or 18° NNW .

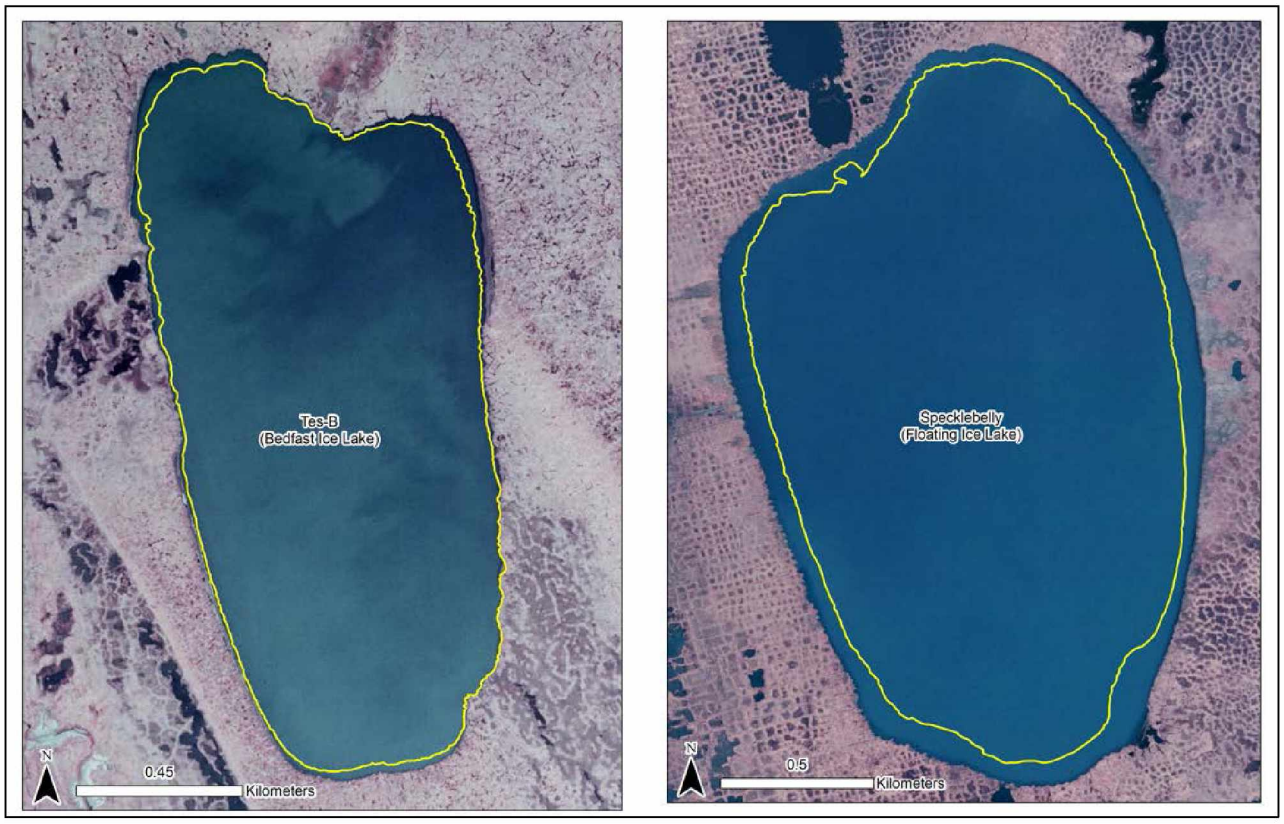

Figure 12: Two lakes within the YOCP, one bedfast (left) and one floating ice (right), show differential shoreline erosion around their perimeters between 1948 and 2002. The pattern for the floating ice lake is more even around the entire perimeter, while the bedfast ice lake shows preferential erosion at the northern and southern ends.

4.4 Changes to Decadal-Scale Thermokarst Lake Expansion Rates

With the addition of the 1979 dataset for some of the lakes within the YOCP, it became clear that among lakes surveyed, expansion rates are elevated for the period of 1979 to 2002 compared to the period or 1948 to 1979 (Figure 13). Overall, for the 6 lakes included in this analysis (3 bedfast and 3 floating), rates increased from 0.53 m/yr to 0.73 m/yr. This pattern was more pronounced in floating ice lakes compared to bedfast ice lakes. In floating ice lakes, the average expansion rates increased by 0.41 m/yr, compared to bedfast ice lakes, which actually decreased in their rate of expansion, by only 0.019 m/yr. This is due to one lake displaying a marked decrease in expansion rate, another seeing almost no change in rate, and a third showing changes more in line with floating ice lakes. The lake that saw a decrease in expansion rate (Tes-B) appears to have had fluctuations in water level which may have obscured detection in this case. In the 2002 imagery, small shelves were exposed on the eastern and western shores of this lake that were not visible in either the 1948 or 1979 imagery, signifying that there was potentially a decrease in water level, either for that specific year or through time. Wadepiper Lake was another lake that, despite increasing slightly in its expansion rate, is expanding so slowly that the changes are below the level of detection. There is also the possibility of a change in water level for Wadepiper; the 1948 imagery appears to have higher water levels than either the 1979 or 2002 imagery, potentially masking a stronger expansion rate signal. This is among the smallest lakes in the study, with among the lowest overall expansion rates. The third bedfast ice lake surveyed for 1979 data did show the increase in expansion rates between the two time periods, but was the largest bedfast ice lake surveyed. For the floating ice lakes, the pattern of increased expansion rates in the more modern time period held across all lakes studied. These lakes are generally sized

the same as those bedfast lakes in the study, with the exception of Tes-001 which is just over 1000 ha in size. Specklebelly and Tes-002 are very similar lakes in size and are in fact quite near each other. Despite the fact that the absolute expansion rates are very dissimilar for these two, likely due to the difference in ice regime, the pattern is the same for both lakes, showing a substantial increase in overall expansion rates between the two time periods. Peatball is the smallest floating ice lake studied, but the expansion rates increased in the period after 1979 similarly to all other floating ice lakes. In fact, each floating ice lake showed an approximate 50% increase in expansion rates in the 1979-2002 period, regardless of the absolute rates observed on these lakes, which vary considerably. This pattern generally agrees with the average trend among all lakes surveyed. The same pattern was not observed for the bedfast ice lakes, where there were essentially three different situations observed.

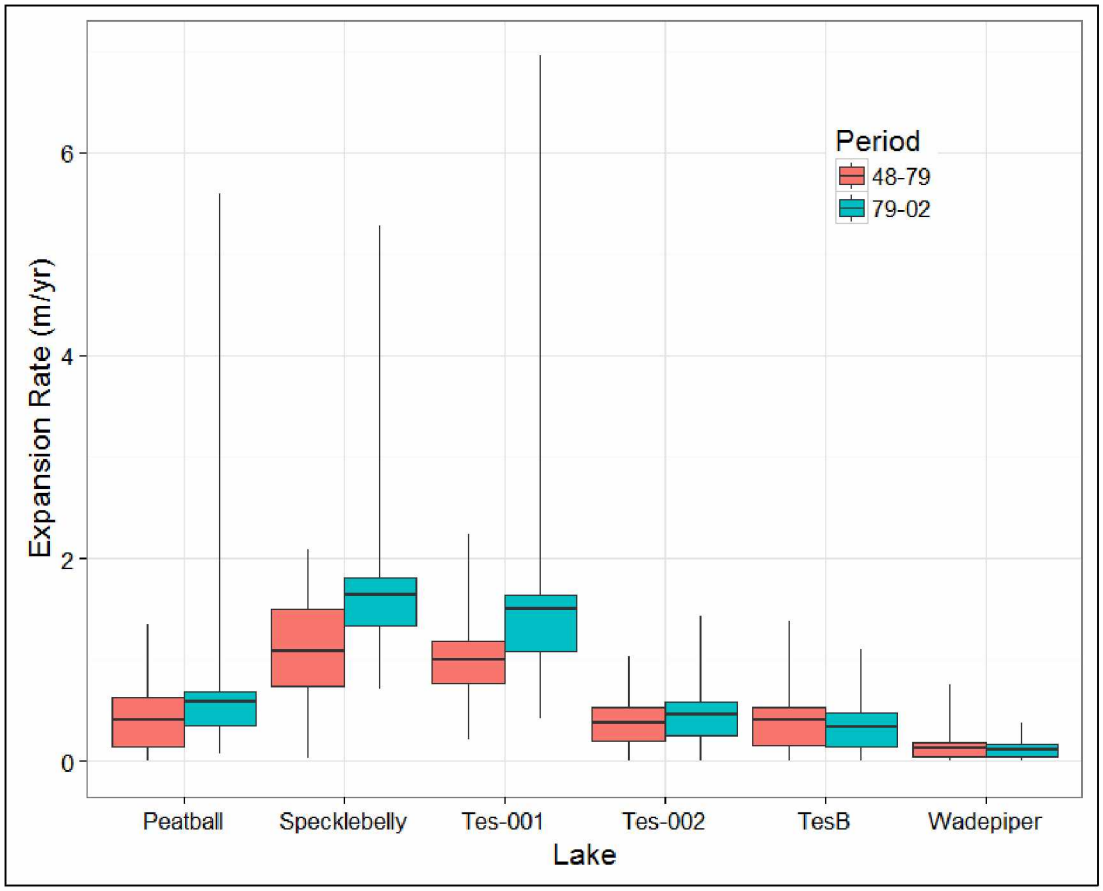

Figure 13: Average expansion rates for 6 lakes within the YOCP for the periods of 1948-1979 and 1979-2002. The boxes represent the 25th to 75th percentile expansion rate, with centerlines as mean expansion rate.

4.5 The Role of Shoreline Terrain Unit on Thermokarst Lake Expansion

Results for expansion rates in different terrain units in the YOCP followed a pattern of areas with low centered polygons and shores only very slightly above lake level having the highest rates of erosion, averaging 130% of whole lake erosion rates (Figure 14). This terrain unit represents the youngest surfaces present within the study area, and is comprised of large, relatively poorly developed low centered polygon surfaces, often inundated for some or all of the erosional season, where the lakes are not ice covered and erosion occurs through thermal and mechanical

action. Those slightly more well defined, slightly older surfaces expressing as either flat center polygons or dry low centered polygons saw erosion rates slightly lower averaging 103% of whole lake erosion rates, and those "primary surfaces" of high centered polygons and lake bluffs several meters above the lake surface level saw the lowest rates of erosion, averaging 88% of whole lake erosion rates. The consistency in these results was not obvious until normalizing the data against the whole lake expansion rates, but then it became clear that almost across all the lakes studied here, the pattern was the same. On both Tes-001 and Specklebelly, it appears that the average rates within the flat centered polygon unit are slightly higher than the rates for the low/inundated polygons. These differences are very slight, however, and within the error range of the dataset. Otherwise the patterns were very similar for all lakes. For those lakes that did not have all three terrain units expressing themselves along their shorelines, the relative patterns remained the same for the two terrain units that were expressed. This means Specklebelly, Wadepiper, and TesB had no primary surface terrain unit along their shorelines, as the primary surface is actually a remnant upland that has not been reworked by past lakeshore expansion and drainage. This remnant upland accounts for only 6% of land area within the YOCP.

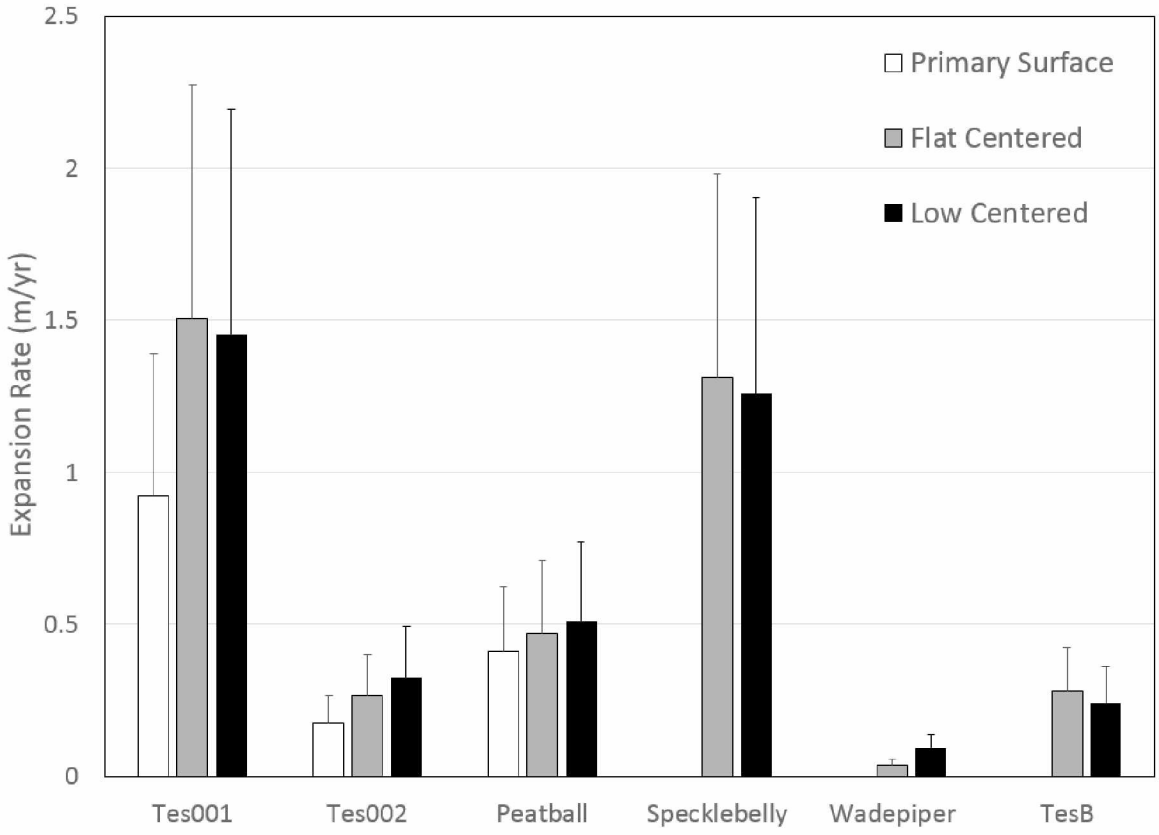

Figure 14: Average expansion rates for 1948-2002 for each of three identified terrain units (Primary surface, flat centered polygons, and low centered polygons). Error bars represent SD.

4.6 Permafrost Characteristics of Various Shoreline Types

Results from samples taken along lake bluffs and from cores were analyzed in the lab for gravimetric moisture content as a proxy for ice content for that sample (Figure 15). There were two sites analyzed for each terrain unit. The two cores taken within the low centered polygon terrain unit, PBC1 and WPC3, showed similar characteristics of extremely high gravimetric moisture contents within the top 50cm of the core. This is due to a high organic content and extremely high ice content. The ice contents drop sharply with depth, and this pattern is consistent for both cores. The two cores within the flat centered polygon terrain unit, WPC1 and PBC2, both

followed similar patterns to the cores taken within the low centered polygon, with high ice contents high in the core and decreasing with depth. A key difference between the two actually ends up being in the location of that ice relative to the level of the lake itself. While the low centered polygons have the areas with the highest ice contents situated very near to the lake level, the flat centered polygons terrain units are set slightly higher above the water surface. The primary surface terrain unit was best assessed through lake bluff exposures rather than through permafrost cores, as the bluffs are too high to effectively represent the conditions along the entire vertical exposure. These samples, too, showed a similar pattern to the cores. Higher in the exposures, the gravimetric moisture contents were much higher, and tapered off with depth. There was significantly more variability in these exposure samples, as well as significantly higher ice contents in the lower parts of the exposure when compared to the lower parts of the core samples. Massive ice bodies were purposefully avoided for sampling, but were mapped. In the exposures on these primary surface lake bluffs, these massive ice bodies can make up a considerable volume of the total bluff. Despite best efforts, none of the samples were taken closer than 1 m above lake level for the lake bluff exposures.

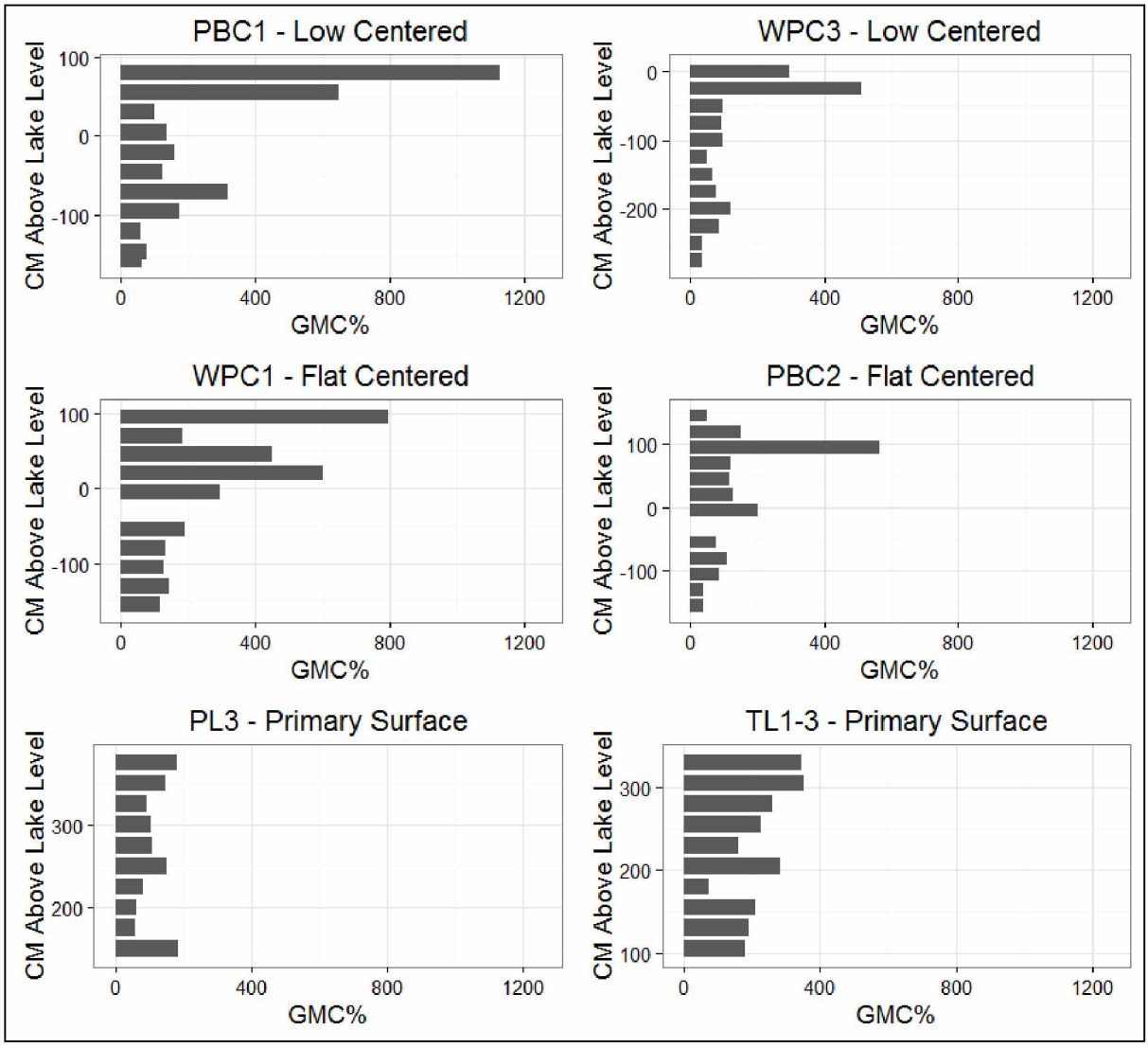

Figure 15: Results of core samples and lake bluff exposure samples from a variety of shoreline types and terrain units in the YOCP, showing increased ground ice contents at different elevations above lake surface level.

4.7 Topography, Thaw Depth, and Ground Thermal Regime of Select Shorelines

Thaw depth measurements within the YOCP conducted in August 2015, near the end of the warming season and near the time of maximum active layer depth, showed patterns across the region. The first pattern was a general increase of thaw depth along the lake shoreline compared to the thaw depth on the adjacent tundra. In general, the taller the lake bluff the more distinct this pattern becomes, with the tallest lake bluffs such as the 4m high bluffs on Peatball Lake having some thaw depths of greater than the 3 meters of probe I carried. In the soil of the YOCP, this could not be an active layer and must be a component of a talik extending laterally into the shoreline. Where lake shorelines are only slightly above the lake level, this effect is less pronounced, with thaw depths more or less consistent across the lengths of the transects. The other major factor for thaw depths apart from shoreline expression is lake ice regime. Despite upland tundra active layer depths being consistent across the study area, floating ice lakes showed thaw depths much deeper, particularly in the shallow littoral zone of the lake. Here depths were often greater than 1m and, again, were in some cases greater than the maximum length of probe at 3m. Bedfast lakes however showed thaw depths only slightly greater than those of the surrounding tundra, being on average 53 cm deep across all surveyed points, whereas the floating ice lakes were on average 68 cm deep across all points surveyed. The deepest thaw depths were recorded along tall lake bluffs for floating ice lakes (Figure 16). Because of the nature of the erosion, these locations often also had the shallowest active layer depths, in locations where thawed material had slumped down and exposed the frozen material.

Temperature data, though limited due to sensor failure, showed much the same patterns as the active layer surveys. The highest temperatures were seen in the near surface sediments in the littoral zones of floating ice lakes. Though a full year was not measured in the location with the

warmest temperatures, the 0.5 m depth thermistor in the littoral zone of Peatball Lake showed higher temperatures than any other location until the sensor failed. The 1m depth in this location recorded a mean annual soil temperature (MAST) of -1.3 °C for the 2015-2016 year, starting in August 2015. This is compared to the temperatures measured at 1m in the tundra in multiple locations showing a MAST on average of -6.8 °C during the same period (Figure 16).

Snow surveys conducted in late April of 2016 showed patterns more related to individual lake morphology than anything else. Where lake bluffs were low, snow depths along the transect perpendicular to the shoreline were similar to the average tundra snow depth. In the YOCP this was around 30-40 cm snow. In cases where the shoreline elevation was less than 50 cm above the lake level, the potential for snow scour was elevated and often led to patches of bare ice adjacent to shore. The opposite is true for those tall bluffs primarily associated with primary surfaces; these tall lake bluffs, up to 4 m in height, collected massive amounts of snow, reaching a maximum snow depth of 177 cm against the tall bluff on Peatball Lake (Figure 16).

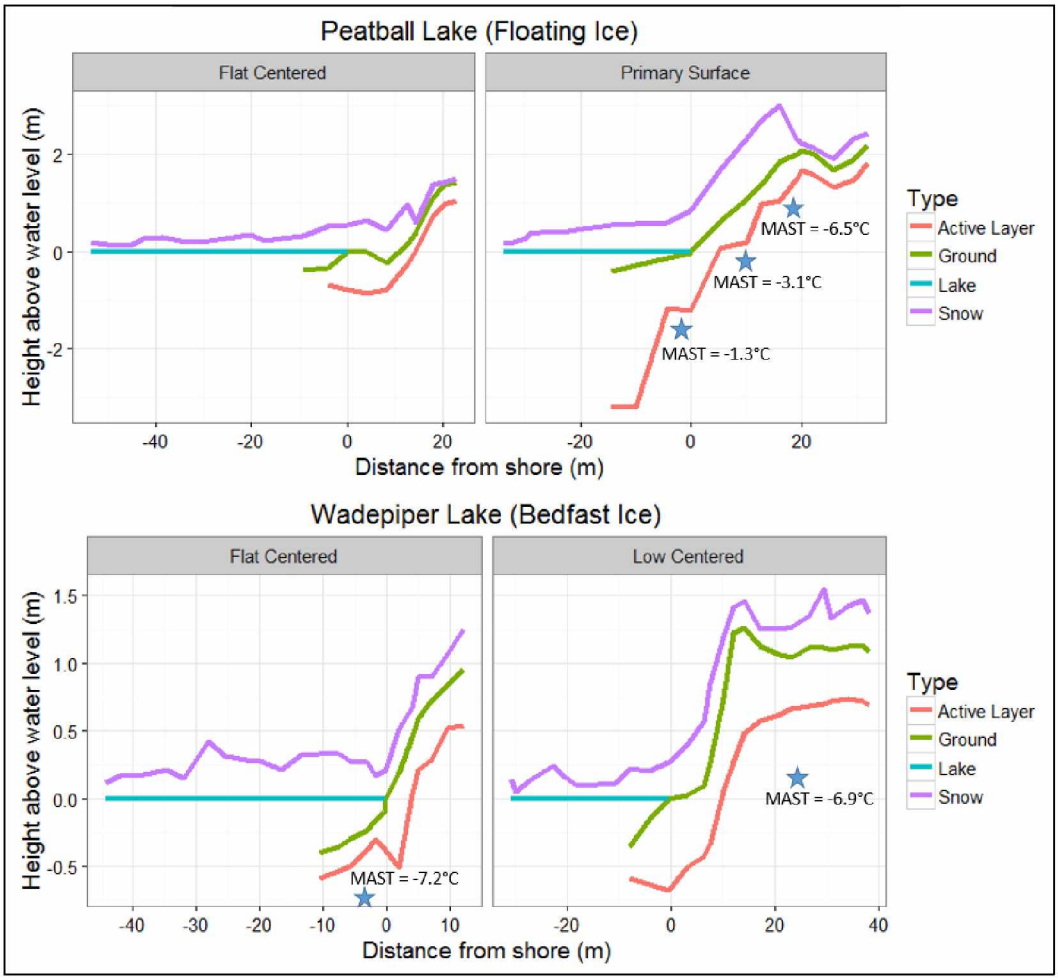

Figure 16: Profiles of ground surface, lake surface, April 2016 snow surface, and August 2015 permafrost table surfaces for different shoreline types and terrain units for two lakes within the YOCP. Stars with captions represent the mean annual soil temperature (MAST) at that location.

4.8 Shoreline Specific Analysis of Erosion Mechanisms

Visits to representative shoreline types (Figure 17) helped to define where each of the different mechanisms of erosion are occurring on a given lake. I visited sites on the ground and observed them via helicopter and found that while erosional processes vary widely across the region, some patterns do begin to emerge. Perhaps the most dramatic form of erosion that occurs on these lakes is that of thermo-erosional niche formation and subsequent block collapse (Figures

18&19). In the visits to lakes I made, nearly all (10 sites out of 11) instances of this type of erosion were visible at the boundaries between different terrain units. The most common (n=7) of these instances occur where a PS unit meets a FC unit. The remainder (n=3) occur where a PS unit meets a LC unit. The final site exhibiting thermo-erosional niche formation was solidly in a FC unit. Within the PS unit itself, the dominant erosional process is that of thermal denudation (Figure 18). These sites exhibit thermally activated and gravity transported mass wasting. A total of 12 sites that were visited were identified as thermal denudation, and all 12 were within PS units. Ice wedge degradation is widespread among lowland units (Figure 19), including LC and FC units identified in the YOCP, and evidence of this process was found on nearly every lake. There were no instances of ice wedge degradation through direct thermal erosion within PS units. The final process discussed, ice shove, is another feature that leaves evidence only in low lying areas (Figure 18). Remnant features where the organic layer was peeled back by ice shove were visible in three locations, each time in conjunction with a low lying area where ice wedge degradation was also occurring.

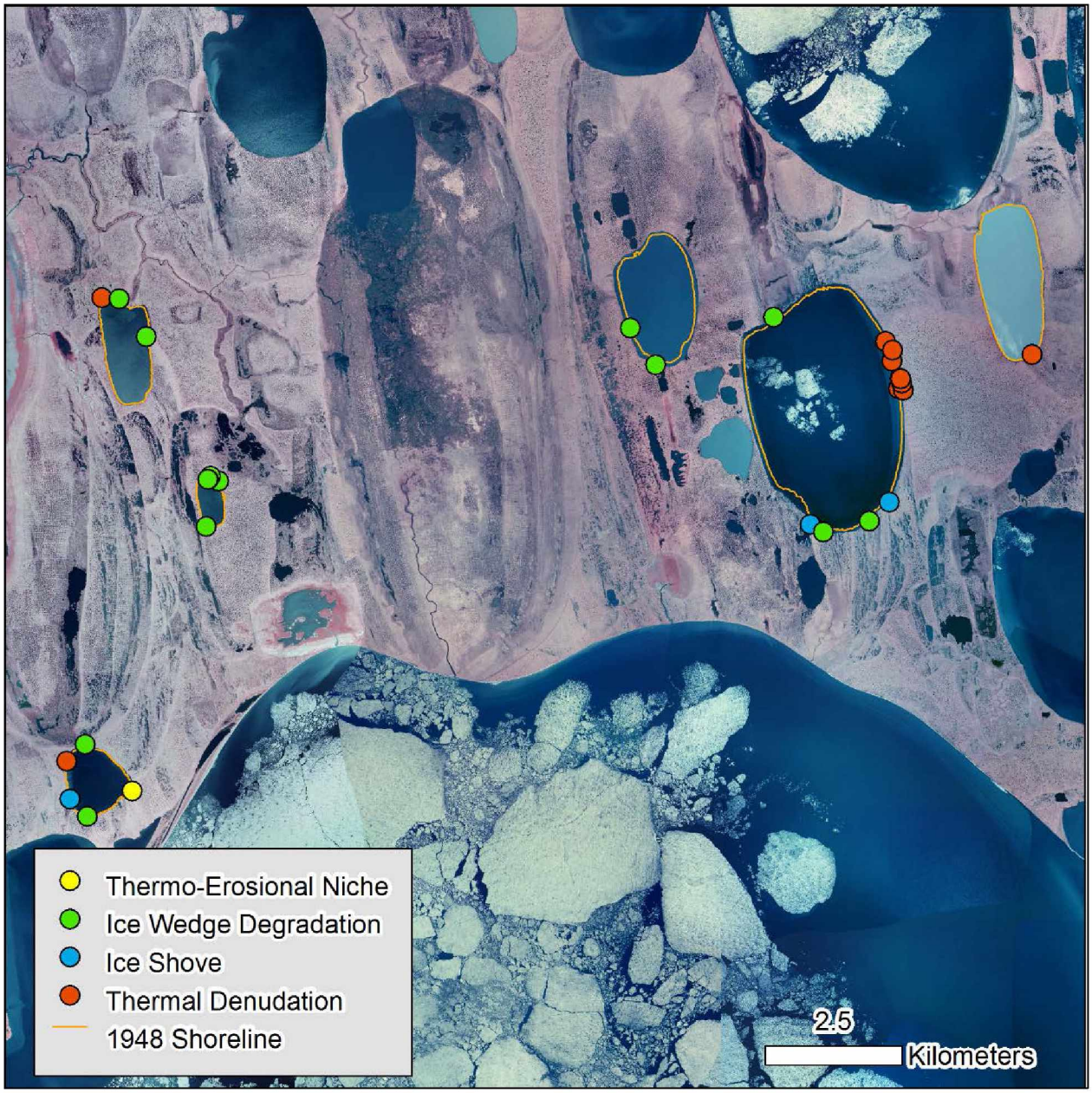

Figure 17: Sites within the YOCP region were visited for qualitative assessment of erosional process.

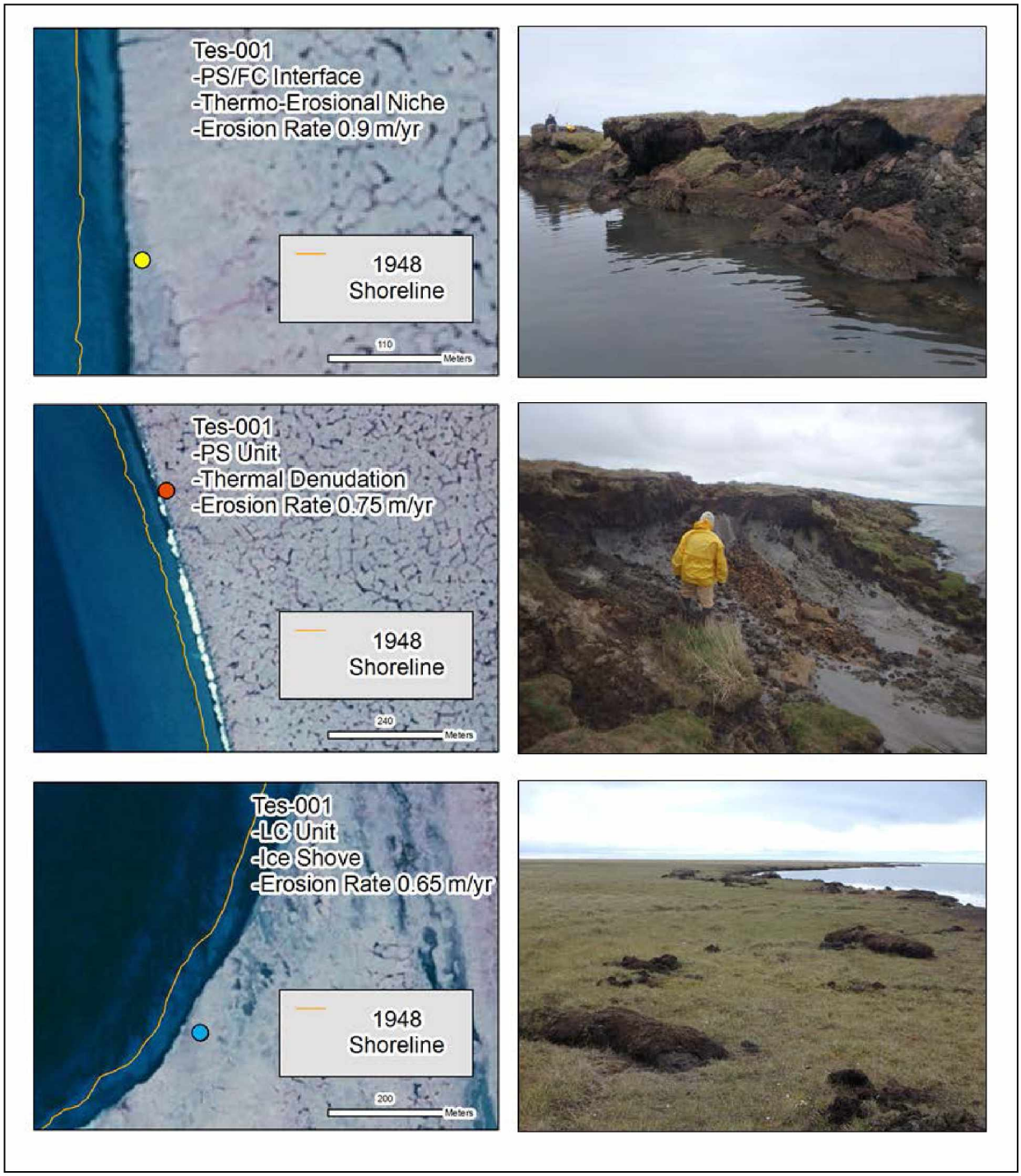

Figure 18: Shoreline erosional processes on Tes-001, including thermo-erosional niches, thermal denudation, and ice shove features.

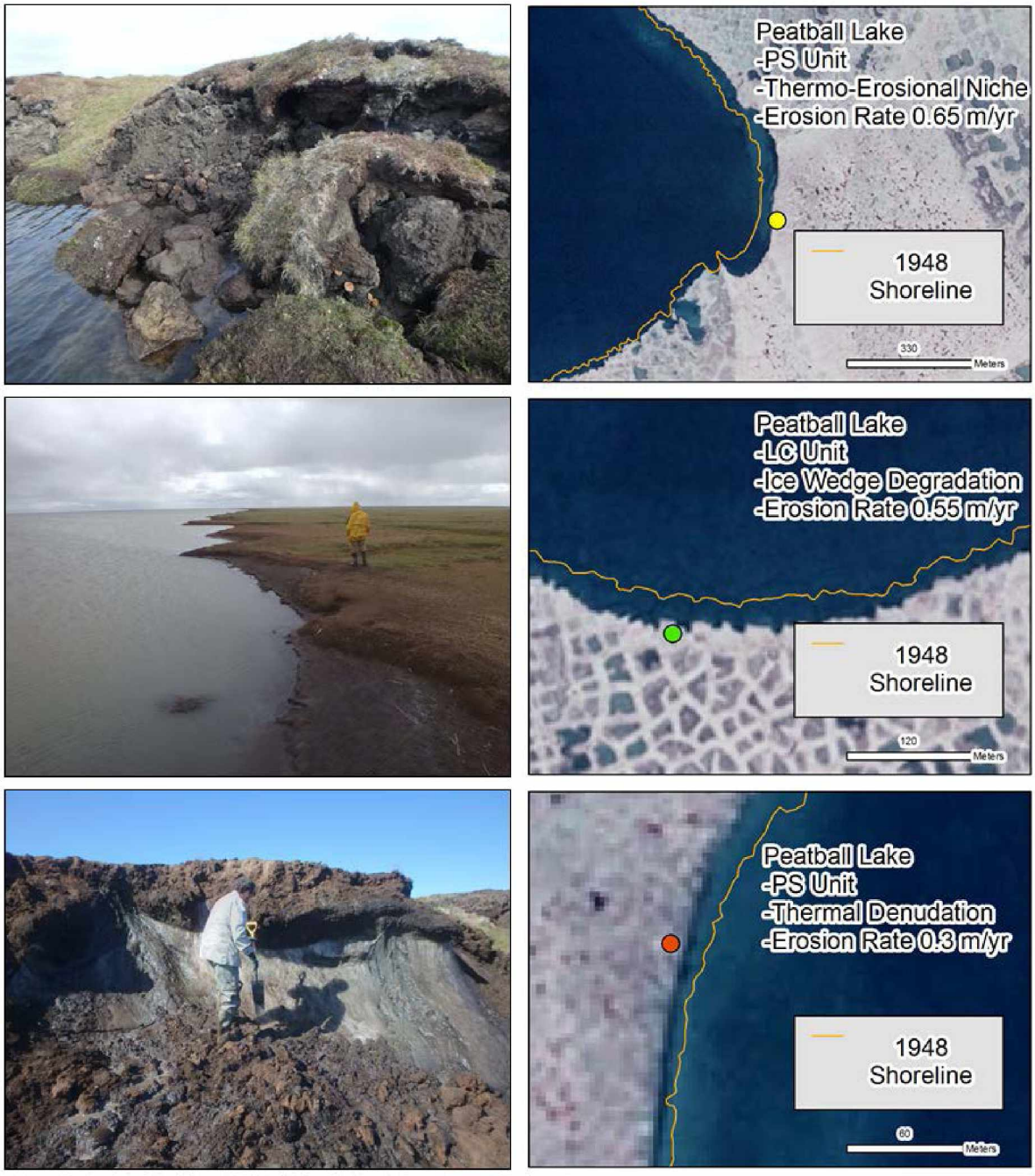

Figure 19: Erosional processes on Peatball Lake, showing thermo erosional niche collapse, ice wedge degradation, and thermal denudation.

5. Discussion

The patterns of lake expansion on the Arctic Coastal Plain of Alaska show clear factors that make lakes and the surrounding areas susceptible to lakeshore erosion. These patterns exist on the broadest spatial scale between the three study regions, down to the finest scale looking at individual shoreline patterns on lakes, and yet there is continuity in many of the identified factors contributing to them. Factors such as near surface geology are important both at the region-wide scale and within individual lakes. The presence or absence of bedfast ice conditions effects expansion rates on an inter-lake scale, as well as on an intra-lake scale where shoreline ice regimes can vary around an individual lake.

5.1 Regional Variation in Lake Expansion

When looking at the broadest scale of observation for this study, I see key differences between each of the three study regions. The YOCP had the highest overall expansion rates, but it also shows the most variability in these rates. Even when normalized by regional average expansion rates, the YOCP had a greater standard deviation than either the OCP or ICP. This is likely due to the heterogeneity of the region. Here we see a landscape that is on the whole younger, with drained thermokarst lake basins of varying ages and sizes across the landscape, and a small percentage of a remnant upland; the terrain unit we call the primary surface. This is, for the most part, a younger landscape than either OCP or the ICP. The fine grained soils deposited 78-59 kya aggraded large quantities of ice quickly, which has allowed for the progression of the thaw lake cycle to alter the landscape into a network of DTLBs and remnant uplands. The young age in conjunction with diversity of landform types likely contribute to the dynamic nature of lakeshore

expansion in this region in particular. The average expansion rate here is likely controlled by the ground ice content. The geomorphic unit of the YOCP has a higher ground ice content than either of the other two regions, making it more susceptible to thermal-mechanical erosion by wave action during the open water season. As the ice in the soil is exposed to warmer temperatures and melts, the subsidence is greater where there is more ice and the soil material that is left behind is more easily transported away from the erosional face due to the fact that there is less material.

The geomorphic unit in OCP is similar in makeup to that of the YOCP, but is a somewhat older surface from a regressive sea. The ice contents there are lower than in the YOCP, but still relatively high (Hinkel et al., 2005). The OCP area is on a very exposed peninsula at the Beaufort and Chukchi seas, and this in combination with the relatively homogenous makeup of the geomorphic unit contribute to its relatively consistent lake sizes and characteristics, including expansion rates and expansion dynamics, potentially contributing to the strong orientation of lakes in this region. If the wind driven lake orientation model (Carson & Hussey, 1962; Hinkel, 2006) is correct, the older ages of these lakes also contributes to this strong orientation, having many years for the wave action to create these shapes. Here, the land is almost entirely reworked by lakes, consisting either of modern day lakes or the remnants of drained thermokarst lake basins. This creates a more homogenous landscape, without the taller lake bluffs seen in the YOCP. The ground ice contents are also typically lower than what is seen in the YOCP. In this case this is not a function of age, but more regional characteristics. This ice content distinction becomes especially important when looking at the ICP. Here, ice contents are substantially lower than in either OCP or the YOCP. This, more than anything else, seems to be the limiting factor to the erosion rates in this region. When the ice within the permafrost along a lakeshore melts, the soils become saturated and more prone to slumping. The volume loss from melted ice can also be a

major factor, particularly in northern Alaska. This can cause thermokarst settlement and slope destabilization, depositing sediment from the lake bluff into the lake below. In the ICP, the relatively ice poor soils are less susceptible to this action as they might be in YOCP or OCP.

When put in the context of prior studies of thermokarst lake expansion rates, the rates reported in this study are comparable to other studies completed on the ACP of Alaska. Lewellen (1970) lists an average erosion rate of 0.73 m/yr in the Barrow Peninsula region, which contains both OCP and YOCP units, and Arp et al. (2011) cite average erosion rates for the Northern TLSA, part of the YOCP, as 0.70 m/yr. This study shows an average rate of 0.57 m/yr for the OCP unit and 0.62 m/yr for the YOCP unit. Jorgenson and Shur (2007) show a mean expansion rate of 0.10 m/yr in the Fish Creek area, part of the ICP, where this study shows an average rate of 0.16 m/yr. This study supports those previous studies, and extends the timeline over which these measurements were taken. The minor variations may be attributed to different lake selection parameters and different data sets and timeline over which the analysis was conducted.

Comparing this study more broadly to other regions with active thermokarst lake activity, we see among the highest rates on the ACP, particularly in the OCP and YOCP units. On the Eastern North Slope of Alaska, Schell and Ziemann (1983) show an average rate of 0.30 m/yr, and on the Northern Seward Peninsula of Alaska, Jones et al. (2011) show an average expansion rate of 0.35 to 0.39 m/yr. These areas have overall lower rates than either the YOCP or the OCP. The interior of Alaska, as reported by Jorgenson and Osterkamp (2005), had expansion rates ranging from 0.10 m/yr to a maximum of 2.0 m/yr; with no average regional rates reported. In the Canadian Yukon territory, near the town of Mayo, lakes are reported by Burn and Smith (1990) as having a mean expansion rates of 0.70 m/yr, but only up to a maximum of 1.2 m/yr. Some lakes in the YOCP have mean expansion rates of greater than this. To the west, in the Northern Hudson Bay

Lowland, Manitoba, Canada, maximum expansion rates are reported as high as 2.0 m/yr, but no average was reported (Dyke and Sladen, 2010). In Sibera, a study by Are et al. (1979) reports mean expansion rates between 0.12 to 0.52 m/yr in central Yakutia, while Tomirdiaro and Ryabchun (1973) report rates of 0.5 to a maximum of 5.0 m/yr on the Anadyr Peninsula. Comparing values reported here to prior work on thermokarst lake expansion shows that lakes on the ACP are dynamic in nature, even in the context of thermokarst lakes as a whole. Rates reported here are consistent with previous studies of the region and show, for the YOCP and OCP units, some of the highest mean expansion rates of thermokarst lakes.

5.2 Lake Morphometric Controls on Expansion

Even within a region, lakes can display a wide range of variability in their expansion rates, due mainly to the lake's own characteristics within the regional setting. One of these factors is lake size; despite several lakes that do not follow the observed pattern, lake size is shown to play a major role in controlling overall lakeshore expansion rates. Particularly within the OCP and YOCP regions, the relationship is quite strong, where average expansion rates increase with lake area. There appears to be both a lower and upper limit to this relationship, where very small lakes (10-75 ha) tend to all have about the same rates and, and the largest lakes (500+ ha) in the study also seem to plateau at an upper expansion rate of about 1.25 m/yr. This is a relationship that may be due to wind fetch; as the lakes increase in size there is a longer area for the size and energy of the waves increase as wind travels across the lake surface. In this relationship, the wave energy on shallower bedfast ice lakes may be depth limited rather than fetch limited. If this is the case, then regardless of lake surface area, these lakes may have a lower maximum wave energy, leading to the lower expansion rates seen in bedfast lakes.

Perhaps the strongest pattern between lakes within a single region ends up being the difference between bedfast and floating ice conditions. In all regions, when whole lake expansion rates are averaged, floating ice lakes are clearly expanding faster than their bedfast ice lake counterparts. Even lakes of the same size in the same region and setting show this pattern of floating ice lakes expanding faster than adjacent bedfast lakes. This difference is likely a combination of factors, but one of the most significant in this region of continuous permafrost is the thermal state under and around a given lake. Where ice freezes to the bed during the winter, the permafrost oftentimes remains intact, and the earlier in a given season this ice freezes to the bed, the colder these permafrost temperatures are going to be. Under a floating ice lake, however, the permafrost thaws through the year, developing a talik underneath the lake and likely extending laterally along the lake bluffs for a short distance. Compared to the bedfast ice lake shorelines, those of the floating ice lake are warmer and less protected from wind driven erosion. The colder temperatures surrounding a bedfast ice lake also protect it from thermal erosion and thermokarst activity in taller bluffs, which can be an effective component of lakeshore expansion. The difference in expansion rates between the two ice regimes is critical in understanding the landscape evolution trajectory for this region of northern Alaska; in a warming arctic climate, many shallow lakes are transitioning from majority bedfast ice to majority floating ice as winter ice growth decreases. This has important implications for lake area change in a region where lakes cover greater than 20% of land area. This shift, in addition to accelerating permafrost thaw beneath the lakes, will also increase the amount of permafrost thawed laterally as the lakes expand.

In addition to the thermal conditions affected by the dichotomy between these two ice regimes, it is important to note the role depth plays. As ice regime and depth are directly related within a single region, bedfast ice lakes also have a different depth regime when compared to

floating ice lakes. The threshold depth for the floating ice lakes is approximately 1.5 m (Brewer, 1958), though can vary based on the ice growth for the year (controlled by temperature and snow depth) and can vary based on local conditions such as topography that may accumulate snow or cause snow scour. Generally, though, in northern Alaska lakes deeper than this tend to be floating ice and shallower tend to be bedfast ice. On larger lakes that have a large wind fetch, this depth may be the limiting factor towards wave development. This would lead to shorter, lower energy waves that are less able to cause erosion on lake shorelines. On smaller lakes, fetch is more likely to be a limiting factor to wave development and cause less of a difference between bedfast and floating ice lakes. Under predicted climate scenarios of thinner lake ice and lakes transitioning from bedfast to floating ice (Arp et al., 2012a; Surdu et al., 2014; Alexeev et al. 2016), lakes will also increase in depth due to volume loss of melting ice in the sublake permafrost. The combination of this increase in depth and transition from bedfast to floating ice lakes may cause many lakes on the ACP to increase their expansion rate.

The theory behind lake orientation proposed by Black and Barksdale (1949) and expanded upon by Carson & Hussey (1962) is supported by this analysis of lakes in the ACP; lakes in the regions of OCP and the YOCP are both shown to expand preferentially in the NW-N direction. This leads to expansion along what is already the long axis of the lake, with significantly lower expansion along the E and W shorelines, reinforcing this orientation over time. Because the land surface in OCP is generally an older unit (Hinkel et al., 2005), this supports the fact that lakes in this region show a stronger orientation, with length to width rations >2, than the YOCP, despite similar expansion dynamics for lakes in each region. Lakes within the YOCP may be expanding at a faster rate along their northern shores, but because they are younger in age, have not yet reached as strong an orientation as seen in OCP. ICP lakes then acts as the counterpoint to these

two groups; because overall expansion rates are lower here, and there are other factors exerting a stronger control than the wind driven orientation theory, these lakes show little to no orientation pattern, with L/W ratios below 1.5. Factors that complicate the analysis of this wind driven orientation theory would include all factors discussed in this study and can alter the expansion dynamics of a lake significantly.

5.3 Shoreline Erosion Processes

The variations on the intra-lake scale mimic those of the regional or inter-lake scale, but with these factors all competing in one lake. This includes late winter ice regime and the condition of the permafrost in this area, differing terrain units around the perimeter of a lake, and even the importance of snow accumulation on lake bluffs. In reference to the late winter ice regime on a lake, it is important to note that any floating ice lake can have sections near the shore where by late winter the ice freezes all the way to the bed, and so it should be expected that the lakeshore expansion rates here would be subject to the same controls that are exerted on bedfast vs floating ice lakes as a whole. The analysis of the ice regime within 100m of shore for these floating ice lakes concludes that yes, where a shoreline is majority bedfast, the expansion rates are lower than on shorelines that are majority floating. This indicates that the dichotomy between these two ice regimes is not simply a function of lake depth, but is linked directly to the ice regime. The fact that permafrost is retained in these bedfast areas is likely the key component to this control. Where the ice freezes to the bed, heat remaining in the sub-lake active layer more easily transmits to the colder air temperatures at the surface. This reduces the depth of thaw and in some cases keeps the permafrost intact, but in all cases keeps the temperatures of the thawed package and permafrost under these regions colder. In areas of bedfast ice, where temperatures are colder, the ground

remains frozen into the summer season and requires more energy to do the work of erosion. In the floating ice shoreline sections, there is liquid water remaining under the lake surface for the entire year, continuing to act as a heat source for the underlying soils. Here, permafrost temperatures are warmer, or more likely, the permafrost has continued to thaw through the winter, creating a situation where summertime erosion can occur much more quickly, requiring less energy to thaw and remove the same amount of material. This can create a pattern of inconsistent erosion around a lake shoreline, driven primarily by the presence of shallow shelves around the lake, which, because of the ice regime, acts as a thermal control on the ground beneath.

Another main factor controlling the differences in expansion rates around the perimeter of a single lake is the setting of that lake. Because of the nature of landscape evolution on the Arctic Coastal Plain, there are distinct terrain units that can differ greatly in their properties and are easily distinguishable with remote sensing techniques. When expansion rates were examined in relation to these terrain unit, an interesting pattern emerged. Despite the older landscape features such as the remnant uplands having a greater amount of ice overall, particularly in the form of massive ice bodies like ice wedges, these features were shown to have slower expansion rates over the period of analysis of this study. This result was somewhat unexpected, partially due to the fact that when viewed at lake level, these taller lake bluffs express themselves as a very dramatic form of erosion. Slope failures and thermally related mass wasting events are common along these shores, and the evidence of this activity is easy to see, with undercut shorelines and exposed ice wedges with unvegetated banks. Shoreline segments with little relief from the lake surface and a younger terrain unit of low centered or flat centered polygons do not have these obvious features of erosion, and instead must incrementally progress throughout the erosional season. The youngest landscape terrain units are shown in this analysis to have the highest expansion rates within the YOCP, but

the evidence is not easy to see except when viewed on the longer timescales of this study. One possible explanation for the discrepancy in what was expected and what is shown to occur is the fact that, although ice contents may be higher overall in the primary surface terrain units, in the low centered and flat centered polygon unit, much of the ice is concentrated very near to the surface. In summer, when the ice in the active layer thaws, these units become vulnerable to erosion. In these places, where ice content can and often does exceed mineral and organic soil, the remaining soil after thaw can easily be reworked and transported away by the wave action of the lake. In contrast, the primary surface unit, which is often expressed as tall bluffs along the lake shore, has a large part of its ice concentrated a meter or more above lake level. In this case, the area that is receiving most of the wave energy from the lake may be primarily mineral soil. While this soil may still be susceptible to mechanical erosion like in any other setting, the lack of the thermal component may slow down the overall rates seen here. Even the thermal erosion that does occur, in the ice rich top section of the exposure, has the potential to limit erosional susceptibilty. As material thaws through air temperature and solar energy, it slides down the slope of the lake bluff and accumulates at the toe of the slope. This addition of material may create a transport limited situation; the wave action cannot keep up with the amount of material being supplied, and can therefore make little to no headway in its effort to erode the shoreline. The combination of these two factors, where the primary surface terrain unit may be both thermal erosion limited and material transport limited, likely leads to the effect of the lowest expansion rates among this terrain unit. In the case of the flat centered polygon terrain unit, it is a mix of both of these situations, where each is mediated by the other and erosion rates are mediated as well.

Field data in this study did not reveal a new understanding of the driving and resisting forces behind lakeshore expansion rates, but rather served to reinforce what has been learned from

remote sensing analysis. Active layer and snow were both surveyed along locations representative of different shoreline types. The data from active layer surveys shows that active layers are generally deeper on the margins of floating ice lakes, regardless of terrain unit. On bedfast ice lakes, however, these active layer depths are similar to depths on the adjacent tundra, and indicate little thermal departure in these shallow water areas.

5.4 Erosion Responses to Changing Climate

From the subset of lakes analyzed with the additional set of 1979 imagery, it seems there is a clear pattern of increased erosion rates, particularly among the floating ice lakes, in the YOCP region. With the effect of arctic amplification warming temperatures in the Arctic faster than at the mid-latitudes, it is appropriate to inspect and expect changes between these two time periods. We have already seen a trend towards warmer temperatures (Hinzman et al., 2005), longer open water seasons, and decreasing annual ice thickness (Arp et al., 2012a, Surdu et al., 2014). The robust temperature record at Barrow, AK shows a marked increase in mean annual air temperature of nearly 3 °C over the period 1979 to 2012 (Wendler et al., 2014). The record in the YOCP and ICP do not extend nearly as long, but they are in similar enough locations that it would be expected they show a similar pattern. Warmer air temperatures could lead to warmer water and soil temperatures during the summer season of erosion. This increase in temperature is one possible explanation for the increased erosion seen in the YOCP, but ground temperatures are not as quick to respond as air temperatures and it is likely this effect would, directly, be small. Another possibility is the longer open water season during the summer that allows for that more days where erosion can occur. As shown by Surdu et al. (2014), lakes on the Arctic Coastal Plain have experienced a decrease in ice cover duration of approximately 24 days over the period from 1950-2011. This significant increase in open water duration likely contributes to the observed increase

in annual lakeshore erosion in this study. The average annual ice thickness is also decreasing through time (Arp et al., 2012a; Surdu et al., 2014; Alexeev et al. 2016), creating a situation where bedfast ice lakes may begin to transition to floating ice lakes. This too would increase average regional expansion rates as lakes shift from the more slowly expanding bedfast ice lakes to the faster expanding floating ice lakes. This same effect may be seen in the nearshore portions of floating ice lakes. Decreasing ice thickness leads to decreased area where lakes may have a bedfast shoreline. This transition to a nearshore floating ice regime would also tend to increase expansion rates in these areas, contributing to an increase in the average whole lake rate. The combination of all of these factors likely leads to the pattern of increased expansion rates in the period from 1979 to 2002 when compared to 1949 to 1979, particularly on the floating ice lakes within the YOCP.

6.0 Conclusions

On the Arctic Coastal Plain of Alaska, lakes are the dominant factors of change across the landscape, due to both their widespread distribution and dynamic nature. For this reason it is imperative to understand the driving and resisting forces at play behind lakeshore expansion. I studied 35 lakes in three regions on the ACP, establishing differential erosion at the regional scale, at the inter-lake scale within a region, and the intra-lake scale, as well as a temporal distribution of two distinct time periods, 1948/49-1979 and 1979-2002 for six lakes. At the regional scale, surface geology and ground ice content are two of the major factors controlling expansion rates, giving each region a distinctly different pattern and amount of erosion. Those areas with the highest ground ice contents (YOCP and OCP) consistently showed higher expansion rates than those relatively ice poor sands in the ICP.

At the inter-lake scale, the two largest factors controlling thermokarst lake expansion appear to be lake surface area and lake ice regime, which is closely related to depth. As lakes increase in size, the increase in wind fetch allows for higher energy in the wave action on the lake, contributing to faster erosion rates on the larger lakes. This effect is mediated to an extent by other factors of the lake, including that lakes ice regime. Across all study areas, floating ice lakes showed increased expansion rates compared to bedfast ice lakes, even at similar lake areas. This is likely due to an armoring effect from the colder permafrost surrounding these lakes; the frozen soils take longer to warm and thaw in the short summer season and therefore are more resistant to mechanical wave action causing shoreline erosion.

At the intra-lake scale, thermokarst lake expansion rates are controlled for the most part by the nearshore bathymetry and corresponding ice regime and the terrain unit type adjacent to a given shore. Nearshore ice regime controls erosion rates in much the same way as it does on a whole lake basis; by armoring the shorelines against thermo-mechanical erosion through colder temperatures. Terrain unit also plays a role in the heterogeneity of erosion around the perimeter of the lake,though the exact mechanism is not exactly clear and may be a combination of factors. One factor is likely the concentration of ground ice near the lake surface in the LC and FC terrain units, therefore making them susceptible to thaw and mechanical erosion through wave action. On the other hand, the PS terrain unit may suffer from a transport limited erosion situation where, despite warmer ground temperatures and increased thaw by the end of the summer, the amount of material introduced by the erosion process may make the shore more resilient to further erosion.

In a changing Arctic climate, understanding the forces shaping the morphology of the ACP becomes increasingly important. With many lakes near the threshold between floating ice and bedfast ice regimes, there may be a widespread transition to more floating ice lakes. As lakes

make this transition, this study shows that we should see a marked increase in lake expansion rates across the region as lakes begin to erode their shores more quickly, and therefore an increase in lake area in general. The sample of lakes within the YOCP show that this increased rate of expansion may already be happening in lakes that have not even undergone an ice regime transition. This has important implications across the Arctic. Increased lakeshore expansion will lead to increased permafrost thaw not just through the formation of sub-lake taliks, but also in the lateral expansion and erosion of material. Through a better understanding of the other factors that influence lakeshore expansion, such as regional to local ground ice contents, lake size, and local bathymetry, we may better predict the changes that will shape the ACP in the years to come.

References

Alerstam, T., G. A. Gudmundsson, M. Green, and A. Hedenström (2001), Migration Along Orthodromic Sun Compass Routes by Arctic Birds, *Science (80-.).*, *291*(5502), 300 LP-303.

Alessa, L., A. Kliskey, R. Lammers, C. Arp, D. White, L. Hinzman, and R. Busey (2008), The arctic water resource vulnerability index: An integrated assessment tool for community resilience and vulnerability with respect to freshwater, *Environ. Manage.*, *42*(3), 523–541, doi:10.1007/s00267-008-9152-0.

Alexeev, V. A., C. D. Arp, B. M. Jones, and L. Cai (2016), Arctic sea ice decline contributes to thinning lake ice trend in northern Alaska, *Environ. Res. Lett.*, *11*(7), 74022, doi:10.1088/1748-9326/11/7/074022.

Are, F. E., V. T. Balobaev, and N. P. Bosikov (1979), Characteristics of the reshaping of shorelines of thermokarst lakes of central Yakutia, Draft Transl. 711, 23 pp., Cold Reg. Res. and Eng. Lab., U.S. Army Corps of Eng., Hanover, N. H.

Arp, C. D., and B. M. Jones (2009), *Geography of Alaska Lake Districts: Identification, Description, and Analysis of Lake-Rich Regions of a Diverse and Dynamic State*. U.S. Geological Survey Scientific Investigations Report 2008-5215, 40p.

Arp, C. D., B. M. Jones, F. E. Urban, and G. Grosse (2011), Hydrogeomorphic processes of thermokarst lakes with grounded-ice and floating-ice regimes on the Arctic coastal plain, Alaska, *Hydrol. Process.*, *25*(15), 2422–2438, doi:10.1002/hyp.8019.

Arp, C. D., B. M. Jones, Z. Lu, and M. S. Whitman (2012a), Shifting balance of thermokarst lake ice regimes across the Arctic Coastal Plain of northern Alaska, *Geophys. Res. Lett.*, *39*(16), doi:10.1029/2012GL052518.

Arp, C. D., M. S. Whitman, B. M. Jones, R. Kemnitz, G. Grosse, and F. E. Urban (2012b), Drainage Network Structure and Hydrologic Behavior of Three Lake-Rich Watersheds on the Arctic Coastal Plain, Alaska, *Source Arctic, Antarct. Alp. Res. Publ. By Inst. Arct. Alp. Res.*, *44*(4), 385–398, doi:10.1657/1938-4246-44.4.385.

Arp, C. D., M. S. Whitman, B. M. Jones, G. Grosse, B. V. Gaglioti, and K. C. Heim (2015), Distribution and biophysical processes of beaded streams in Arctic permafrost landscapes, *Biogeosciences*, *12*(1), 29–47, doi:10.5194/bg-12-29-2015.

Arp, C. D., B. M. Jones, G. Grosse, A. C. Bondurant, V. E. Romanovsky, K. M. Hinkel, and A. D. Parsekian (2016), Threshold sensitivity of shallow Arctic lakes and sublake permafrost to changing winter climate, *Geophys. Res. Lett.*, *43*(12), 6358–6365, doi:10.1002/2016GL068506.

Berkes, F., and D. Jolly (2002), Adapting to Climate Change: Social-Ecological Resilience in a Canadian Western Arctic Community, *Ecol. Soc.*, *5*.

Billings, W. D., and K. M. Peterson (1980), Vegetational Change and Ice-Wedge Polygons through the Thaw-Lake Cycle in Arctic Alaska, *Arct. Alp. Res.*, *12*(4), 413–432, doi:10.2307/1550492.

Black, R. F., and W. L. Barksdale (1949), Oriented Lakes of Northern Alaska, *J. Geol.*, *57*(2), 105–118.

Bowling, L. C., D. L. Kane, R. E. Gieck, L. D. Hinzman, and D. P. Lettenmaier (2003), The role of surface storage in a low-gradient Arctic watershed, *Water Resour. Res.*, *39*(4), doi:10.1029/2002WR001466.

Boyd, W. L. (1959), Limnology of Selected Arctic Lakes in Relation to Water Supply Problems, *Ecology*, *40*(1), 49–54, doi:10.2307/1929921.

Brewer, M. C., L. D. Carter, and R. Glenn (1993), No Title, in *Proceedings of the Sixth International Conference on Permafrost*, pp. 48–53, South China University of Technology Press, Beijing, China.

Brewer, M. C. (1958), The thermal regime of an Arctic lake, *Eos, Trans. Am. Geophys. Union*, *39*(2), 278–284, doi:10.1029/TR039i002p00278.

Britton, M. E. (1957), Vegetation of the arctic tundra, in *Arctic Biology*, edited by H. P. Hansen, pp. 67–113, Oregon State University Press, Corvallis, Oregon.

Brown, J., Radiocarbon Dating, Barrow, Alaska (1965), *Arctic*, *18*, 37–48, doi:10.2307/40507337.

Burn, C. R., and M. W. Smith (1990), Development of thermokarst lakes during the holocene at sites near Mayo, Yukon territory, *Permafr. Periglac. Process.*, *1*(2), 161–175, doi:10.1002/ppp.3430010207.

Burn, C. R., and M. W. Smith (2006), Development of thermokarst lakes during the holocene at sites near Mayo, Yukon territory, *Permafr. Periglac. Process.*, *1*(2), 161–175, doi:10.1002/ppp.3430010207.

Cabot, E. C. (1947), The Northern Alaskan Coastal Plain Interpreted from Aerial Photographs, *Geogr. Rev.*, *37*(4), 639–648, doi:10.2307/211190.

Carson, C. E. (1968), Radiocarbon Dating of Lacustrine Strands in Arctic Alaska, *Arctic*, *21*(1), 12–26.

Carson, C. E., and K. M. Hussey (1962), The Oriented Lakes of Arctic Alaska, *J. Geol.*, *70*(4), 417–439.

Carter, L. D. (1981), A Pleistocene sand sea on the Alaskan Arctic coastal plain. *Science*, 211: 381–383.

Carter, L.D., Brouwers, E.M., and Marincovich, Louie, Jr. (1988), Nearshore marine environments of the Alaskan Beaufort Sea during deposition of the Flaxman Member of the Gubik Formation, in Galloway, J.P., and Hamilton, T.D., eds., Geologic studies in Alaska by the U.S. Geological Survey during 1987: U.S. Geological Survey Circular 1016, p. 27-30.

Dinter, D. A., L. D. Carter, and J. Brigham-Grette (1990), Late Cenozoic geologic evolution of the Alaskan North Slope and adjacent continental shelves, in The Geology of North America, vol. I, *The Arctic Ocean Region*, edited by A. Grantz et al., pp. 459 – 490, Geol. Soc. of Am., Boulder, Colo.

Dmitriev, E. M., and O. N. Tolstikhin (1971), Use of Groundwater for Water Supply in the Yakutian ASSR: Prospects, Exploration and Extraction, *Якутск ИМЗ СО РАН*.

Dyke, L. D., and W. E. Sladen (2010), Permafrost and Peatland Evolution in the Northern Hudson Bay Lowland, Manitoba, *ARCTIC*, *63*(4), 429–441, doi:10.14430/arctic3332.

Everdingen, R. O. van (1998), *Glossary of Permafrost and Related Ground-Ice Terms*, 2nd ed., Calgary, Alberta, CANADA.

Everett, K. R. (1980), Landforms, in *Geobotanical Atlas of the Prudhoe Bay Region, Alaska*, edited by D. A. Walker, pp. 14–19, U.S. Army Cold Regions Research and Engineering Laboratory, Hanover, N.H.

Farquharson, L., D. H. Mann, G. Grosse, B. M. Jones, and V. E. Romanovsky (2016), Spatial distribution of thermokarst terrain in Arctic Alaska, *Geomorphology*, *273*, 116–133, doi:10.1016/j.geomorph.2016.08.007.

Grosse, G., B. Jones, and C. Arp (2013), 8.21 Thermokarst Lakes, Drainage, and Drained Basins A2 - Shroder, John F. BT - Treatise on Geomorphology, pp. 325–353, Academic Press, San Diego.

Hamilton, T. D. (1965), Alaskan Temperature Fluctuations and Trends: An Analysis of Recorded Data, *Arctic*, *18*, 104–117, doi:10.2307/40488297.

Hapke, C. J. (2005), Estimation of regional material yield from coastal landslides based on historical digital terrain modelling, *Earth Surf Process. Landforms*, *30*(6), 679–697, doi:10.1002/esp.1168.

Heinke, G. W., and B. Deans (1973), Water supply and waste disposal systems for Arctic communities, *Arctic*, *62*, 149–159.

Hinkel, K. (2006), Comment on "Formation of oriented thaw lakes by thaw slumping" by Jon D. Pelletier, *J. Geophys. Res. Earth Surf.*, *111*(F1), n/a-n/a, doi:10.1029/2005JF000377.

Hinkel, K. M., W. R. Eisner, J. G. Bockheim, F. E. Nelson, K. M. Peterson, and X. Dai (2003), Spatial Extent, Age, and Carbon Stocks in Drained Thaw Lake Basins on the Barrow Peninsula, Alaska, *Arctic, Antarct. Alp. Res.*, *35*, 291–300, doi:10.2307/1552564.

Hinkel, K. M., R. C. Frohn, F. E. Nelson, W. R. Eisner, and R. A. Beck (2005), Morphometric and spatial analysis of thaw lakes and drained thaw lake basins in the western Arctic Coastal Plain, Alaska, *Permafr. Periglac. Process.*, *16*(4), 327–341, doi:10.1002/ppp.532.

Hinkel, K. M., B. M. Jones, W. R. Eisner, C. J. Cuomo, R. A. Beck, and R. Frohn (2007), Methods to assess natural and anthropogenic thaw lake drainage on the western Arctic coastal plain of northern Alaska, *J. Geophys. Res. F Earth Surf.*, *112*(2), doi:10.1029/2006JF000584.

Hinkel, K. M., Y. Sheng, J. D. Lenters, E. A. Lyons, R. A. Beck, W. R. Eisner, and J. Wang (2012), Thermokarst Lakes on the Arctic Coastal Plain of Alaska: Geomorphic Controls on Bathymetry, *Permafr. Periglac. Process.*, *23*(3), 218–230, doi:10.1002/ppp.1744.

Hinzman, L. D. et al. (2005), Evidence and Implications of Recent Climate Change in Northern Alaska and Other Arctic Regions, *Clim. Change*, *72*(3), 251–298, doi:10.1007/s10584-005-5352-2.

Hopkins, D. M. (1949), Thaw Lakes and Thaw Sinks in the Imuruk Lake Area, Seward Peninsula, Alaska, *J. Geol.*, *57*(2), 119–131.

Jeffries, M. O., K. Morris, and G. E. Liston (1996), A Method to Determine Lake Depth and Water Availability on the North Slope of Alaska With Spaceborne Imaging Radar and Numerical Ice Growth Modelling, *Arctic*, *49*(4), 367–374.

Jones, B. M., C. D. Arp, M. T. Jorgenson, K. M. Hinkel, J. A. Schmutz, and P. L. Flint (2009), Increase in the rate and uniformity of coastline erosion in Arctic Alaska, *Geophys. Res. Lett.*, *36*(3), n/a-n/a, doi:10.1029/2008GL036205.

Jones, B. M., G. Grosse, C. D. Arp, M. C. Jones, K. M. Walter Anthony, and V. E. Romanovsky (2011), Modern thermokarst lake dynamics in the continuous permafrost zone, northern Seward Peninsula, Alaska, *J. Geophys. Res. Biogeosciences*, *116*(G2), n/a-n/a, doi:10.1029/2011JG001666.

Jones, B. M., and C. D. Arp (2015), Observing a Catastrophic Thermokarst Lake Drainage in Northern Alaska, *Permafr. Periglac. Process.*, *26*(2), 119–128, doi:10.1002/ppp.1842.

Jones, B. M., C. D. Arp, K. M. Hinkel, R. A. Beck, J. A. Schmutz, and B. Winston (2009), Arctic Lake Physical Processes and Regimes with Implications for Winter Water Availability and Management in the National Petroleum Reserve Alaska, *Environ. Manage.*, *43*(6), 1071–1084, doi:10.1007/s00267-008-9241-0.

Jorgenson, M. T., and J. Brown (2005), Classification of the Alaskan Beaufort Sea Coast and estimation of carbon and sediment inputs from coastal erosion, *Geo-Marine Lett.*, *25*(2), 69–80, doi:10.1007/s00367-004-0188-8.

Jorgenson, M. T., and T. E. Osterkamp (2005), Response of boreal ecosystems to varying modes of permafrost degradation, *Can. J. For. Res.*, *35*(9), 2100–2111, doi:10.1139/x05-153.

Jorgenson, M. T., and Y. Shur (2007), Evolution of lakes and basins in northern Alaska and discussion of the thaw lake cycle, *J. Geophys. Res. Earth Surf.*, *112*(F2), doi:10.1029/2006JF000531.

Kanevskiy, M., Y. Shur, M. T. Jorgenson, C.-L. Ping, G. J. Michaelson, D. Fortier, E. Stephani, M. Dillon, and V. Tumskoy (2013), Ground ice in the upper permafrost of the Beaufort Sea coast of Alaska, *Cold Reg. Sci. Technol.*, *85*, 56–70, doi:http://dx.doi.org/10.1016/j.coldregions.2012.08.002.

Kobayashi, N. (1985), Formation of thermoerosional niches into frozen bluffs due to storm surges on the Beaufort Sea coast, *J. Geophys. Res. Ocean.*, *90*(C6), 11983–11988, doi:10.1029/JC090iC06p11983.

Kokelj, S. V, T. C. Lantz, J. Kanigan, S. L. Smith, and R. Coutts (2009), Origin and polycyclic behaviour of tundra thaw slumps, Mackenzie Delta region, Northwest Territories, Canada, *Permafr. Periglac. Process.*, *20*(2), 173–184, doi:10.1002/ppp.642.

Kovacs, A. (1983), *Shore ice ride-up and pile-up features, Part I: Alaska's Beaufort Sea coast*, United States Army Cold Regions Research Engineering Laboratory, Hanover N.H.

Lachenbruch, A. H., M. C. Brewer, G. W. Greene, and B. V. Marshall (1962), Temperatures in permafrost, *Temp. - Its Meas. Control Sci. Ind.*, *3*, 791–803.

Langer, M., S. Westermann, J. Boike, G. Kirillin, G. Grosse, S. Peng, and G. Krinner (2016), Rapid degradation of permafrost underneath waterbodies in tundra landscapes—Toward a representation of thermokarst in land surface models, *J. Geophys. Res. Earth Surf.*, *121*(12), 2446–2470, doi:10.1002/2016JF003956.

Lantuit, H., and W. H. Pollard (2008), Fifty years of coastal erosion and retrogressive thaw slump activity on Herschel Island, southern Beaufort Sea, Yukon Territory, Canada, *Geomorphology*, *95*(1–2), 84–102, doi:http://dx.doi.org/10.1016/j.geomorph.2006.07.040.

Leffingwell, E. de K. (1915), Ground-Ice Wedges: The Dominant Form of Ground-Ice on the North Coast of Alaska, *J. Geol.*, *23*, 635–654, doi:10.2307/30062549.

Lehner, B., and P. Döll (2004), Development and validation of a global database of lakes, reservoirs and wetlands, , doi:10.1016/j.jhydrol.2004.03.028.

Lewellen, R. I. (1970), Permafrost Erosion Along the Beaufort Sea Coast, 25 pp., Univ. of Denver, Denver.

Ling, F., and T. Zhang (2003), Numerical simulation of permafrost thermal regime and talik development under shallow thaw lakes on the Alaskan Arctic Coastal Plain, *J. Geophys. Res. Atmos.*, *108*(D16), doi:10.1029/2002JD003014.

Livingstone, D. A. (1954), On the orientation of lake basins [Alaska], *Am. J. Sci.* , *252*(9), 547–554, doi:10.2475/ajs.252.9.547.

Mackay, J. R. (1970), Disturbances to the tundra and forest tundra environment of the western Arctic, *Can. Geotech. J.*, *7*(4), 420–432, doi:10.1139/t70-054.

Mackay, J. R. (1988), Catastrophic lake drainage, Tuktoyatuk Peninsula area, District of Mackenzie, *Curr. Res. Part D. Geol. Surv. Canada*, 83–90.

Mackay J.R. (1992), Lake stability in an ice-rich permafrost environment: examples from the Western Arctic Coast. In Arctic Ecosystems in semi-arid regions: Implications for Resource management, Robarts RD, Bothwell ML (eds). National Hydrology Research Institute Symposium Series 7, Environment Canada, Saskatoon: Saskatchewan; 1–25.

Marsh, P., M. Russell, S. Pohl, H. Haywood, and C. Onclin (2009), Changes in thaw lake drainage in the Western Canadian Arctic from 1950 to 2000, *Hydrol. Process.*, *23*(1), 145–158, doi:10.1002/hyp.7179.

Martin, D., D. Bélanger, P. Gosselin, J. Brazeau, C. Furgal, and S. Déry (2007), Drinking Water and Potential Threats to Human Health in Nunavik: Adaptation Strategies under Climate Change Conditions, *Arctic*, *60*(2), 195–202.

O'Sullivan, J. B. (1961), Quaternary geology of the Arctic coastal plain, northern Alaska, Ph.D. dissertation, Iowa State Univ. Sci. and Technol., Ames.

Raynolds, M.K., Walker, D.A., Maier, H.A. (2006), Alaska Arctic Tundra Vegetation Map. 1:4,000,000. U.S. Fish and Wildlife Service. Anchorage, AK.

Roulet, N. T., and M.-K. Woo (1988), Runoff generation in a low Arctic drainage basin, *J. Hydrol.*, *101*(1–4), 213–226, doi:10.1016/0022-1694(88)90036-4.

Roy-Léveillée, P., and C. R. Burn (2017), Near-shore talik development beneath shallow water in expanding thermokarst lakes, Old Crow Flats, Yukon, *J. Geophys. Res. Earth Surf.*, *122*(5), 1070–1089, doi:10.1002/2016JF004022.

Rovansek, R. J., L. D. Hinzman, and D. L. Kane (1996), Hydrology of a Tundra Wetland Complex on the Alaskan Arctic Coastal Plain, U.S.A., *Arct. Alp. Res.*, *28*(3), 311, doi:10.2307/1552110.

Schell, D. M., and P. J. Ziemann (1983), Accumulation of peat carbon in the Alaska Arctic Coastal Plain and its role in biological productivity, in Fourth International Conference on Permafrost, edited by T. L. Pewe and J. Brown, pp. 1105–1110, Natl. Acad. Press, Fairbanks, Alaska

Sellmann, P. V., J. Brown, R. I. Lewellen, H. McKim, and C. Merry (1975), *The classification and geomorphic implications of thaw lakes on the Arctic coastal plain, Alaska.* CRREL Research Report 344, 21pp., United States Army Cold Regions Research Engineering Laboratory, Hanover N.H.

Serreze, M. C., J. E. Walsh, F. S. Chapin Iii, T. Osterkamp, M. Dyurgerov, V. Romanovsky, W. C. Oechel, J. Morison, T. Zhang, and R. G. Barry (2000), OBSERVATIONAL EVIDENCE OF RECENT CHANGE IN THE NORTHERN HIGH-LATITUDE ENVIRONMENT, *Clim. Chang.*, *46*, 159–207.

Shelesnyak, M. C. (1948), Arctic Research Laboratory, Office of Naval Research, Point Barrow, Alaska, *Science (80-.).*, *107*(2777).

Shulski, M., and G. Wendler (2007), *The climate of Alaska*, University of Alaska Press.

Sibley, P. K., D. M. White, P. A. Cott, and M. R. Lilly (2008), Introduction to Water Use From Arctic Lakes: Identification, Impacts, and Decision Support1, *JAWRA J. Am. Water Resour. Assoc.*, *44*(2), 273–275, doi:10.1111/j.1752-1688.2007.00159.x.

Sturm, M., and G. E. Liston (2003), The snow cover on lakes of the Arctic Coastal Plain of Alaska, U.S.A, *J. Glaciol.*, *49*, 370–380.

Surdu, C. M., C. R. Duguay, L. C. Brown, and D. F. Prieto (2014), Response of ice cover on shallow lakes of the North Slope of Alaska to contemporary climate conditions (1950–2011): radar remote-sensing and numerical modeling data analysis, *Cryosph.*, *8*, 167–180, doi:10.5194/tc-8-167-2014.

Thieler, E. R., E. A. Himmelstoss, J. L. Zichichi, and A. Ergul (2009), Digital Shoreline Analysis System (DSAS) version 4.0—An ArcGIS extension for calculating shoreline change, U.S. Geol. Survey Open File Rep., 2008–1278.

Tomirdiaro, S. V., and V. K. Ryabchun (1973), Lake thermokarst on the Lower Anadyr Lowland, in Permafrost: USSR Contribution to the Second International Conference, Yaktusk, USSR, pp. 94–100, Natl. Acad. Sci., Washington, D. C

Urban, F. E., and G. D. Clow (2015), DOI/GTN-P climate and active-layer data acquired in the National Petroleum Reserve - Alaska and the Arctic National Wildlife Refuge, 1998-2013,

Vincent, W. F., and J. E. Hobbie (2000), Ecology of Arctic lakes and rivers, in *The Arctic: Environment, People and Policy*, edited by M. Nuttal and T. V. Callaghan, pp. 197–274, Overseas Publishers Association, Amsterdam.

Walter, K. M., S. A. Zimov, J. P. Chanton, D. Verbyla, and F. S. Chapin (2006), Methane bubbling from Siberian thaw lakes as a positive feedback to climate warming, *Nature*, *443*(7107), 71–75.

Wendler, G., L. Chen, and B. Moore (2014), Recent sea ice increase and temperature decrease in the Bering Sea area, Alaska, *Theor. Appl. Climatol.*, *117*, 393–398, doi:10.1007/s00704-013-1014-x.

West, J. J., and L. J. Plug (2008), Time-dependent morphology of thaw lakes and taliks in deep and shallow ground ice, *J. Geophys. Res. Earth Surf.*, *113*(F1), n/a-n/a, doi:10.1029/2006JF000696.

Williams, J. R. (1983), Engineering-geologic maps of northern Alaska, Meade River quadrangle, *U.S. Geol. Surv. Open File Rep.*, 83-294.

Williams, J. R., Carter, L. D., and Yeend, W. E. (1978): Coastal plain deposits of the NPRA. In Johnson, K. (ed.), The United States Geological Survey in Alaska: accomplishments during 1977. U.S. Geological Survey Circular 772-B: 20–22.

Zimov, S. A., Y. V Voropaev, I. P. Semiletov, S. P. Davidov, S. F. Prosiannikov, F. S. Chapin, M. C. Chapin, S. Trumbore, and S. Tyler (1997), North Siberian Lakes: A Methane Source Fueled by Pleistocene Carbon, *Science (80-.).*, *277*(5327), 800 LP-802.